

Bistability of prefrontal states gates access to consciousness

Highlights

- vIPFC recordings during visual rivalry reveal frontal dynamics of conscious access
- Update and stability of conscious content in a tug of war between distinct LFP bands
- Changes in the encoding of conscious contents follow an increase in 1–9 Hz activity
- Content-agnostic prefrontal fluctuations gate sensory access to consciousness

Authors

Abhilash Dwarakanath, Vishal Kapoor,
Joachim Werner, Shervin Safavi,
Leonid A. Fedorov,
Nikos K. Logothetis,
Theofanis I. Panagiotaropoulos

Correspondence

abhilash.dwarakanath@tuebingen.mpg.de (A.D.),
theofanis.panagiotaropoulos@tuebingen.mpg.de (T.I.P.)

In brief

Mesoscale ensemble recordings in the vIPFC during no-report binocular rivalry show that stochastic prefrontal state fluctuations are associated with spontaneous changes in the content of consciousness. Transitions from beta band to low-frequency field activity precede both spontaneous changes in perception and encoding of the contents of consciousness by competing neuronal ensembles. Temporal dynamics of prefrontal state fluctuations during awake resting state mimic the temporal dynamics of binocular rivalry, suggesting a causal role in perceptual multistability.

Article

Bistability of prefrontal states gates access to consciousness

Abhilash Dwarakanath,^{1,4,6,*} Vishal Kapoor,^{1,5,6} Joachim Werner,¹ Shervin Safavi,^{1,2} Leonid A. Fedorov,¹ Nikos K. Logothetis,^{1,3,5,7} and Theofanis I. Panagiotaropoulos^{1,4,7,8,*}

¹Department of Physiology of Cognitive Processes, Max Planck Institute for Biological Cybernetics, Tübingen 72076, Germany

²International Max Planck Research School, Tübingen 72076, Germany

³Division of Imaging Science and Biomedical Engineering, University of Manchester, Manchester M13 9PT, UK

⁴Cognitive Neuroimaging Unit, Institut National de la Santé et de la Recherche Médicale, Commissariat à l'Energie Atomique et aux énergies alternatives, Université Paris-Saclay, NeuroSpin Center, 91191 Gif-sur-Yvette, France

⁵International Center for Primate Brain Research, Center for Excellence in Brain Science and Intelligence Technology (CEBSIT), Chinese Academy of Sciences, Shanghai, China

⁶These authors contributed equally

⁷Senior author

⁸Lead contact

*Correspondence: abilash.dwarakanath@tuebingen.mpg.de (A.D.), theofanis.panagiotaropoulos@tuebingen.mpg.de (T.I.P.)

<https://doi.org/10.1016/j.neuron.2023.02.027>

SUMMARY

Access of sensory information to consciousness has been linked to the ignition of content-specific representations in association cortices. How does ignition interact with intrinsic cortical state fluctuations to give rise to conscious perception? We addressed this question in the prefrontal cortex (PFC) by combining multi-electrode recordings with a binocular rivalry (BR) paradigm inducing spontaneously driven changes in the content of consciousness, inferred from the reflexive optokinetic nystagmus (OKN) pattern. We find that fluctuations between low-frequency (LF, 1–9 Hz) and beta (~20–40 Hz) local field potentials (LFPs) reflect competition between spontaneous updates and stability of conscious contents, respectively. Both LF and beta events were locally modulated. The phase of the former locked differentially to the competing populations just before a spontaneous transition while the latter synchronized the neuronal ensemble coding the consciously perceived content. These results suggest that prefrontal state fluctuations gate conscious perception by mediating internal states that facilitate perceptual update and stability.

INTRODUCTION

When the visual system is confronted with ambiguous sensory information, conscious perception spontaneously fluctuates between different possible perceptual interpretations.¹ In a stochastic manner, one of the competing representations temporarily gains access to consciousness while the others become perceptually suppressed, therefore dissociating sensory input from subjective conscious perception. This perceptual multistability is a gateway in understanding the mechanism that mediates the emergence of visual consciousness, due to the spontaneous switching of conscious perception between different co-registered representations.^{2–5}

Multistable visual perception, in particular binocular rivalry (BR), has been combined with direct neuronal recordings in the non-human primate (NHP) brain to study the neuronal correlates of consciousness (NCC). During BR, the content of consciousness spontaneously alternates between two disparate stimuli that are continuously presented to each eye.^{6–8} Neurons that correlate with the content of consciousness in BR should fire

more when their preferred stimulus is perceptually dominant and decrease their firing when it is perceptually suppressed, therefore providing an explicit representation of conscious contents. NHP electrophysiological studies have shown that such explicit representations are more reliably observed in association cortical areas like the prefrontal cortex (PFC) and temporal cortex compared with early visual areas.^{9–14} However, the exact neural mechanisms underlying the spontaneously driven passage of sensory input from non-conscious processing to conscious access, and vice versa, remain largely unknown.¹⁵ Understanding the mechanisms of spontaneous switching between different conscious contents could provide general insights for the emergence of conscious perception in the brain. In particular, the spontaneous nature of perceptual transitions in multistable perception could reveal the interplay between global cortical state fluctuations, which occur spontaneously during wakefulness and reflect fluctuations in internal states like arousal or attention,^{16–22} and the local ignition of content-selective neuronal representations, which has been associated with the access of sensory information to consciousness.^{23–25}

Two mechanisms associated with different cortical areas have been proposed to drive the spontaneous transitions in conscious content during BR: competition between monocular neurons (i.e., eye-specific input) in the primary visual cortex (V1) and a selection process between stimulus representations in higher-order associational cortical areas, in particular the PFC and parietal cortex (PPC).^{26–29} The originally proposed mechanism that involves competition among monocular V1 neurons may not be sufficient to explain rivalrous switches in conscious perception.¹³ This is because BR involves competition among higher-order perceptual representations of the rivaling stimuli that are not bound to eye-specific input,³⁰ and the percentage of neurons that correlate with conscious perception is higher in associational cortical areas.¹¹ By contrast, monocular neurons in V1 continue to fire, even when their preferred stimulus is perceptually suppressed.¹³ Moreover, switches in the activity of ocular dominance columns during BR can be observed in V1 during anesthesia³¹ or for invisible patterns,³² suggesting a dissociation of neural activity and consciousness in V1.

The second candidate mechanism that involves an active selection process among the rivaling stimulus representations in the PFC,^{1,33,34} where the contents of consciousness can be decoded from neuronal population activity,^{9,10,35} has not been systematically explored. This may possibly be implemented through spontaneous fluctuations in cortical states that modulate the ignition of content-specific neuronal representations in the PFC and therefore access of these representations to consciousness.^{36–39}

The concept of ignition is central to the global neuronal workspace theory (GNWT) of consciousness, which posits that access to consciousness is mediated by non-linear amplification (i.e., ignition) of neuronal activity in association cortical areas like the PFC and PPC. Ignition can be thought to result in crossing a threshold⁴⁰ that allows the broadcast of sensory information to widely distributed cortical networks,^{24,27} thus allowing it conscious access. Ignition associated with conscious perception has been classically observed as a sudden and sustained non-linear increase in gross-scale brain activity measured by functional magnetic resonance imaging (fMRI), electroencephalography (EEG), electrocorticography (ECoG), and magnetoencephalography (MEG), around 200–300 ms after the onset of stimuli that are consciously perceived.^{23,24,41–44} At the neuronal level, evidence for ignition comes from studies showing an amplification of activity in the frontal, parietal, somatosensory, and ventral premotor cortices at the single neuronal level, when sensory information enters consciousness.^{34,45}

Interestingly, the propagation of stimulus-driven activity from lower visual areas to the PFC, where (together with the PPC) the ignition of content-selective representations determines conscious access of sensory input, is influenced by the amplitude of global pre-stimulus states of neural activity.³⁴ Intuitively, such pre-stimulus states, known to fluctuate due to variability in internal states like arousal or attention,^{16,19} can be understood as reflecting a gating mechanism: an operation that could potentially control the threshold to conscious perception. For example, gating could be implemented through the bistability of intrinsically generated cortical states suggested to mediate active maintenance and update of information in the cortex.⁴⁶

However, to date, there is scant evidence as to what cortical states are the substrates of prefrontal gating that regulate ignition and enable access to consciousness.

In the present study, we attempted to unravel the mechanisms underlying the emergence of conscious perception in the macaque lateral PFC, using a no-report BR paradigm.⁹ This paradigm allowed us to detect internally driven transitions in the conscious perception of stimuli that moved in opposing directions. We combined this task with multi-electrode recordings of local field potentials (LFPs) and simultaneously sampled direction-of-motion-selective spiking activity of competing neuronal ensembles. By using the optokinetic nystagmus (OKN) reflex as an objective criterion of perceptual state transitions, we removed any effects of voluntary motor reports on neural activity, thus identifying signals directly related to spontaneous transitions in the content of consciousness.

Our results suggest that spontaneously occurring, ongoing alternations in the prefrontal state between low-frequency (LF) (1–9 Hz) and beta (20–40 Hz) activity directly relate to the update and stability of prefrontal representations of conscious contents, respectively. We show that the amplitude of these LFP fluctuations in the PFC is content agnostic and precede both spontaneous OKN changes (signaling transitions in the content of consciousness) during BR and spontaneous ignitions of conscious contents, indicating that PFC activity is not a mere consequence of conscious perception. Furthermore, we find that these global fluctuations are also modulated on a local level through interactions with content-selective populations that depend on the activity state of these populations and therefore the perceptual dominance or suppression of their preferred stimulus. These results suggest that waking LFP state fluctuations in the PFC have a regulatory role in the ignition of conscious content representations within the same area, acting as a gate to conscious access.

RESULTS

We performed multi-electrode extracellular recordings of LFPs and direction-of-motion-selective neuronal ensembles in the inferior convexity of the macaque PFC (Figure 1A). The inferior convexity of the macaque ventrolateral PFC (vPFC) is homologous to the human inferior frontal gyrus and has direct anatomical connections to the PPC,^{47,48} thus forming the “frontoparietal loop,” which is hypothesized to control access to consciousness.²⁷ Two trial conditions were employed: (1) physical alternation (PA) of monocularly alternating gratings with opposing directions of motion and (2) BR, where the initial direction of motion stimulus was not removed but was followed by a grating moving in the opposite direction, presented to the contralateral eye (Figure 1B). This manipulation results in an externally induced period of perceptual suppression for the first stimulus of variable duration (binocular flash suppression [BFS]), which is then followed by spontaneous perceptual transitions, since the two competing representations (upward vs. downward direction of motion) start to rival for access to consciousness. In order to exclude the effect of voluntary perceptual reports on neural activity, the macaques were not trained to report their percept. Instead, the polarity of their motion-induced OKN elicited during passive observation of the stimuli, which was previously shown to

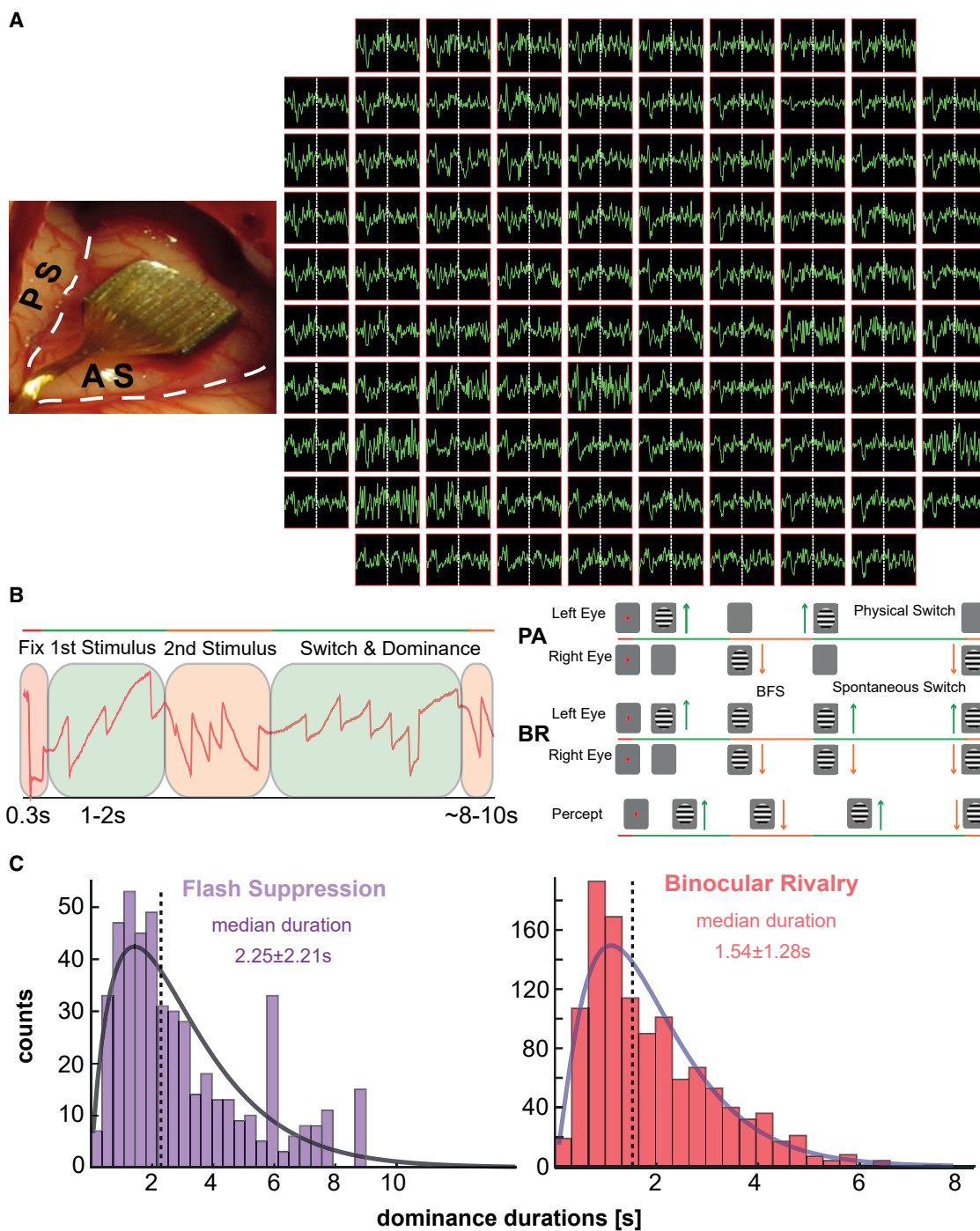


Figure 1. Experiment and typical LFP signals

(A) Multi-electrode array in the inferior convexity of the PFC (top). AS, arcuate sulcus; PS, principal sulcus. Below, an example spatial map of 0.1–250 Hz LFP signals around a change in the OKN polarity (white line) signaling a spontaneous perceptual transition.

(B) Task structure: in BR trials, after an initial phase of BFS, the two competing stimuli rivaled for 8–10 s, eliciting different OKN patterns (red trace, highlighted in green and orange). In PA, the stimuli were alternated monocularly.

(C) Perceptual dominance durations during BFS and BR switches estimated from the OKN follow a classical gamma distribution.

provide an accurate (and faster, compared with manual responses) perceptual state readout in both humans and macaques,^{49–53} was used to infer perceptual dominance periods (**Figure 1B**). Here, by perceptual dominance periods, we mean periods for which perception was stable for one or the other stimulus, based on the OKN readout. These dominance durations followed a gamma distribution, a hallmark of multistable perception,^{1,54,55} with a median dominance duration of 1.54 ± 1.28 s (median \pm SD) for spontaneous transitions in BR and 2.25 ± 2.21 s for transitions involving exogenous perceptual suppression in BFS (**Figure 1C**).

Prefrontal state fluctuations precede spontaneous changes in conscious perception

To investigate the role of internal cortical states in the update and stability of conscious perception, we first analyzed LFP activity dynamics to identify mesoscopic signal fluctuations occurring around periods of externally induced (PA) and spontaneous (BR) perceptual transitions (**Figures 2A** and **S1**). Transient negative deflections of the channel-averaged, raw LFPs (0.1–250 Hz, blue traces in **Figure 2A**) were observed to disrupt activity in the beta range (20–40 Hz) throughout the observation periods in both PA and BR trials. However, the strongest negative deflections appeared to occur after the change in the OKN polarity, induced by external stimulus changes in PA (**Figure 2A**, left), but before the change in the OKN polarity that signals spontaneous perceptual transitions in BR (**Figure 2A**, right). The negative deflections were associated with increases in low-frequency (1–9 Hz, LF) activity (**Figure 2A**, bottom raw; blue vs. purple traces).

In individual BR transitions, a LF-associated beta (20–40 Hz) suppression started clearly before the spontaneous OKN change that signals a perceptual change (**Figure 2B**, right), but it manifested itself after the stimulus and OKN change in PA transitions (**Figure 2B**, left). Pooling all physical stimulus transitions in PA ($n = 1,322$) revealed that an increase in the LF power was concentrated immediately after exogenous stimulus changes and was also accompanied by a temporally transient suppression of the ongoing beta activity (**Figure 2C**, left). The LF-associated beta suppression was also observed for intrinsically generated perceptual transitions in BR ($n = 573$); however, it started well before (~400 ms) the spontaneous OKN change (**Figure 2C**, right). Due to the spontaneous nature of perceptual transitions in BR, the absence of a feedforward response, locked to an external change of the sensory input as in PA, resulted in a temporal jitter of the LF transients across different transitions (data not shown). However, spectrograms aligned to the LF event peaks detected before and after the OKN transitions in BR and PA, respectively, show a similarity in the coupling of LF activity and beta-burst suppression between the two conditions (**Figure S2**). Therefore, these results show that suppression of 20–40 Hz activity during 1–9 Hz transients follows exogenous stimulus changes in PA but precedes spontaneous OKN-inferred perceptual transitions in BR.

To clarify the relationship between the observed broadband transients (negative or positive) and the observed LF bumps in the spectrograms, we first computed the wavelet power spectrum around transitions. The normalized power spectrum (**Figure 3A**) before a spontaneous transition revealed a strong bump in the

beta range (20–40 Hz), indicating periodic, sustained oscillatory activity. The power in the LF band was weaker, yet deviated from a typical 1/f spectrum, thereby casting doubt on its oscillatory vs. aperiodic nature. To resolve this, we also treated the activity in LF as aperiodic and detected events in the same way. We then compared the timings of the detected broadband negative (and positive) transients and the detected LF events, as coincidences per time bin, approaching a transition. We find that these LF events are strongly correlated with negative broadband deflections, as compared with the positive transients (**Figures 3B** and **3C**), both in number and in time approaching a switch. Therefore, in all further analysis, we concentrate on the events and activity in this 1–9 Hz band, and resort to periodic analysis because simple event-based analysis is not amenable to answer complex questions of potential spike-LFP coding mechanisms.

First, we quantified the event rate of LF and beta activity, before and after the time of exogenous (PA) and endogenous (BR) perceptual transitions (described in STAR Methods; only the event rates for LF are reported). LF event rate (events/transitions/channel) was significantly higher after the OKN change in PA (0.36 ± 0.0046 , $n = 46,495$ events, post-transition, vs. 0.09 ± 0.0014 , pre-transition, $n = 11,330$ events; $p < 10^{-187}$ mean \pm SEM; unless specified), but before the OKN change in BR (0.17 ± 0.002 , $n = 9,670$ events, pre-transition vs. 0.14 ± 0.002 , $n = 7,734$ events, post-transition; $p < 10^{-43}$ mean \pm SEM) (**Figure 4A**). Furthermore, the LF events occurred significantly more often before a spontaneous perceptual transition in BR than before a physical transition in PA (0.17 ± 0.002 , $n = 9,670$, pre-transition BR vs. 0.09 ± 0.0014 , $n = 11,330$, pre-transition PA; $p < 10^{-150}$). To understand the marginal (in value) yet significant difference between the average LF event time, before and after the spontaneous perceptual transitions in BR, one must consider that a post-switch period in BR could be in many instances the pre-switch period of the subsequent transition. To understand this relationship further, we discarded events occurring 250 ms after the OKN change, as this period encompasses the mean visually evoked potential (VEP) time in PA when aligned to the actual stimulus onset. After this correction, LF events occurred at -114 ± 190 ms (**Figure S4**, top row), thus further enhancing the pre- vs. post-switch difference.

Importantly, LF events occurred on average even before the end of the last OKN/perceptual dominance period preceding a spontaneous BR transition (end of perceptual dominance: -97.4 ± 140 ms, LF events collected up to the beginning of the next transition: -198 ± 133 ms, [median \pm SD] $p < 10^{-67}$, **Figure 4B**; see **Figure 4B** for an example transition). As expected, LF events occurred predominantly and significantly after the OKN change in PA (64 ± 147 ms). When these PA switches were aligned to the visual stimulus onset, the event times were further shifted (190 ± 162 ms, **Figure S3** middle row shows that the average latency between the physical stimulus onset and the change in the OKN is 190 ± 36.5 ms).

LF activation before a spontaneous perceptual switch in BR could also be observed in the evolution of event rate in time (quasi-peristimulus [event] time histogram [PSTH], to obtain an events/second/transition measure; **Figure 4C**). In BR, the peak rate of LF events occurred at -160 ± 237 ms and -28 ± 199 ms before the spontaneous perceptual transitions for the two

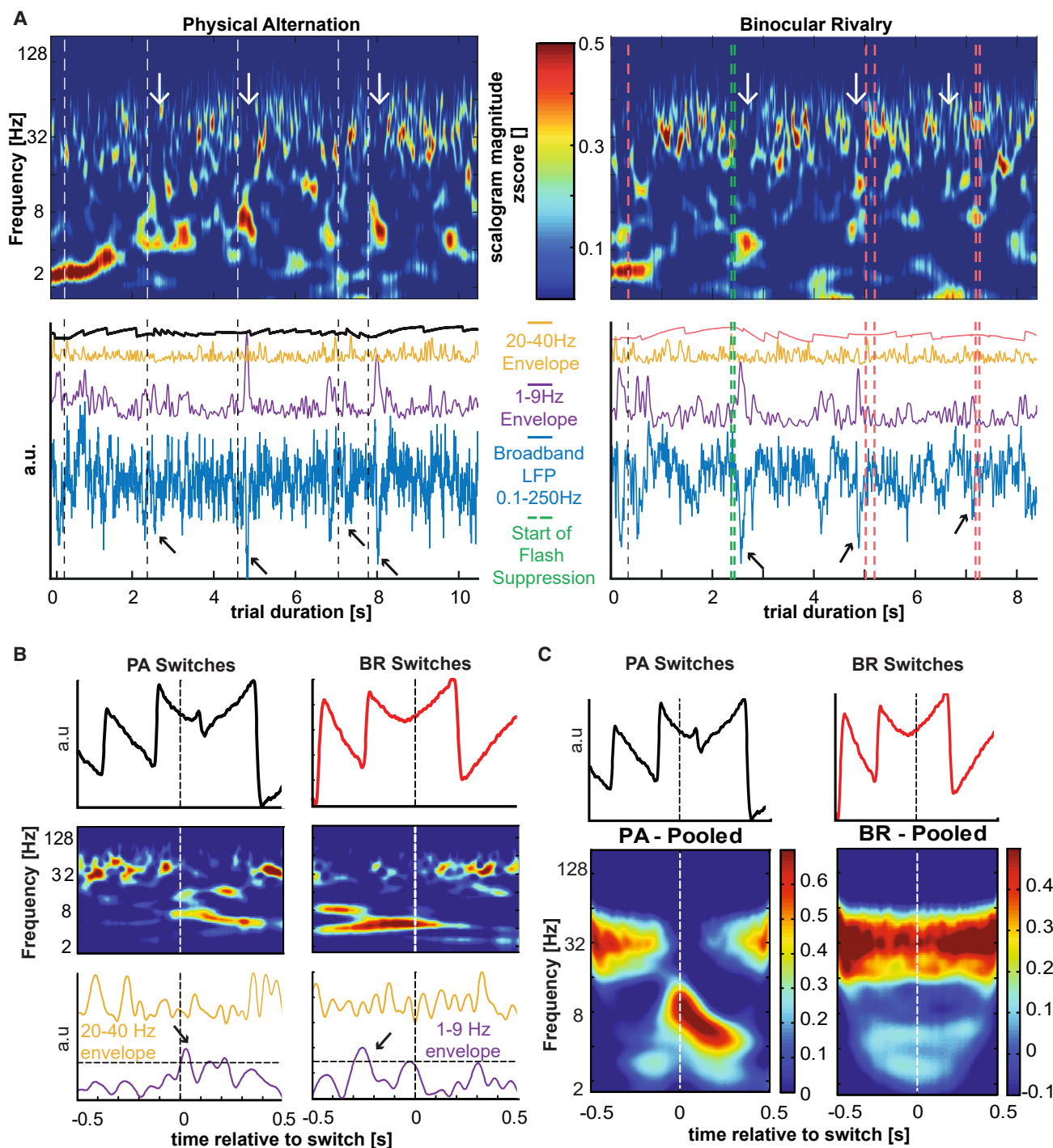


Figure 2. Time-frequency LFP analysis

(A) Z-scored scalograms for a single trial/observation period of PA (left) and BR (right) are shown at the top. White lines in PA reflect the manually marked change in the OKN polarity. Green lines in BR represent the start of the flash suppression phase, and red lines represent the subsequent spontaneous perceptual transitions. LF events occur after a switch in PA but before a switch in BR (white arrows). Bottom panels: broadband LFP (blue), LF amplitude (purple), beta-band amplitude (orange) and corresponding OKN traces. Black arrows point to negative deflections in the broadband trace.

(B) Upper panel: OKN traces around a single physical (black) and spontaneous (red) transition. Middle panel: Z-scored scalograms aligned to the OKN slope change for the two conditions. Lower panel: normalized instantaneous amplitudes of LF (purple) and beta (orange) activity.

(C) Grand average time-frequency analysis of spontaneous transitions (right) and an equal number of randomly sampled physical (left) and transitions. (Colorbar has the same units as A).

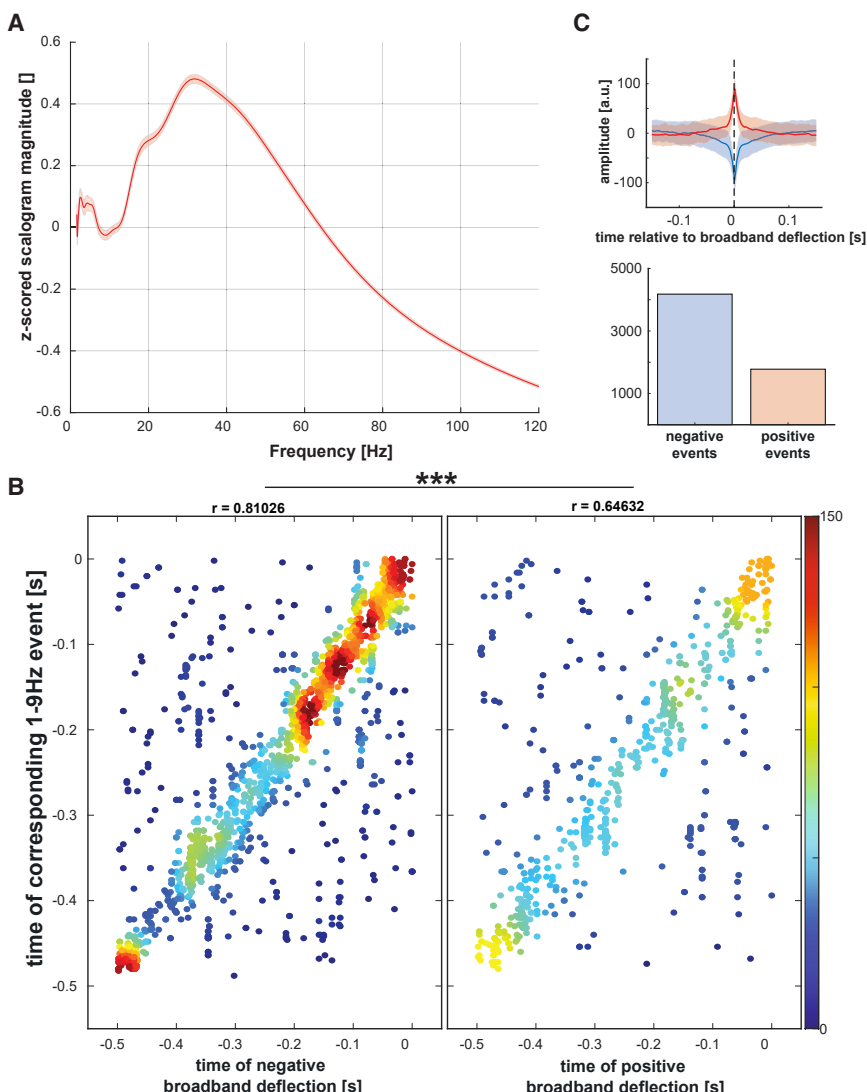


Figure 3. Correlation between 1–9 Hz events and negative broadband deflections

(A) Time-collapsed Z-scored scale-spectrum shows strong oscillatory activity in the beta band (center frequency of ~30 Hz) and weak, quasi-oscillatory/aperiodic activity in LF.

(B) Temporal coincidence density estimate between the detected LF events and negative broadband deviations yields a stronger correlation between LF events and negative transients, than with positive transients. The coincidence per bin for negative transients increases as one approaches a spontaneous switch in time.

(C) Mean positive and negative broadband deflection waveforms and their prevalence.

that in many instances before a spontaneous transition, the last transient LF (1–9 Hz) event was frequently preceded by similar but of lower amplitude events (Figures 5A and S1). Fitting a line to the relationship between the transition-averaged LF event amplitudes at every time point before a transition revealed a linearly increasing relationship between the two variables before a spontaneous (adjusted $R^2 = 0.34$) but not before a physical switch (adjusted $R^2 = -0.003$) (Figure 5B). Next, we asked if there is a similar increase in the spatial pattern of LF amplitude increase during the period approaching an OKN change/perceptual switch. We counted the number of channels displaying instantaneous power in the LF band higher than the array mean (in 25 ms bins). Indeed, after a very brief non-linear increase, the number of participating sites increases linearly, approaching a switch (Figure 5C). Taken

transition types, respectively (Figure 4C, top row), while in PA it occurred at 52 ± 28 ms and 82 ± 64.5 ms following the marked OKN change (Figure 4C, bottom row). Confirming the time-frequency analysis pattern in Figure 2A and suggesting a frequency-specific competitive process (i.e., cortical state fluctuations) in the PFC, the LF and beta event rates were significantly anti-correlated in BR ($r = -0.08$, $p = 0.0071$; pooled across both transition types; Figure 4D). We confirmed the significance of this negative correlation value by shuffling the beta amplitude at LF peak rate 1,000 times. The mean Pearson's correlation coefficient was no different from zero, with a p value of 0.493 (Figure S3, bottom row), suggesting that the small but negative correlation value is biologically relevant.

Spatiotemporal buildup of LF prefrontal activity

Are the LFP events preceding a spontaneous change in the content of consciousness, random large excursions from baseline activity, or do they reflect a gradual buildup process that is critical for inducing a spontaneous transition? Indeed, we noticed

together, these results indicate the occurrence of a mesoscopic, spatiotemporal spread of LF prefrontal events before spontaneous perceptual reversals operating at a linear scale.

LF activity is stronger before spontaneous transitions toward a clear percept

We further hypothesized that if an increase in LF activity is critical for inducing spontaneous perceptual reversals, then this activity should be significantly weaker when perceptual transitions were not complete but resulted in piecemeal (PM) periods. PM periods were detected in periods that the OKN did not change polarity after the end of a dominance period, therefore indicating that following the OKN change, perception did not unambiguously favor either of the two competing directions of motion. Subtracting the time-frequency decomposition of transitions to a PM percept from that of clean BR perceptual transitions revealed a preponderance of LF activity before a switch (Figure 6A). Additionally, the LF event rate was higher before a clear spontaneous transition compared with the period before transition to a PM

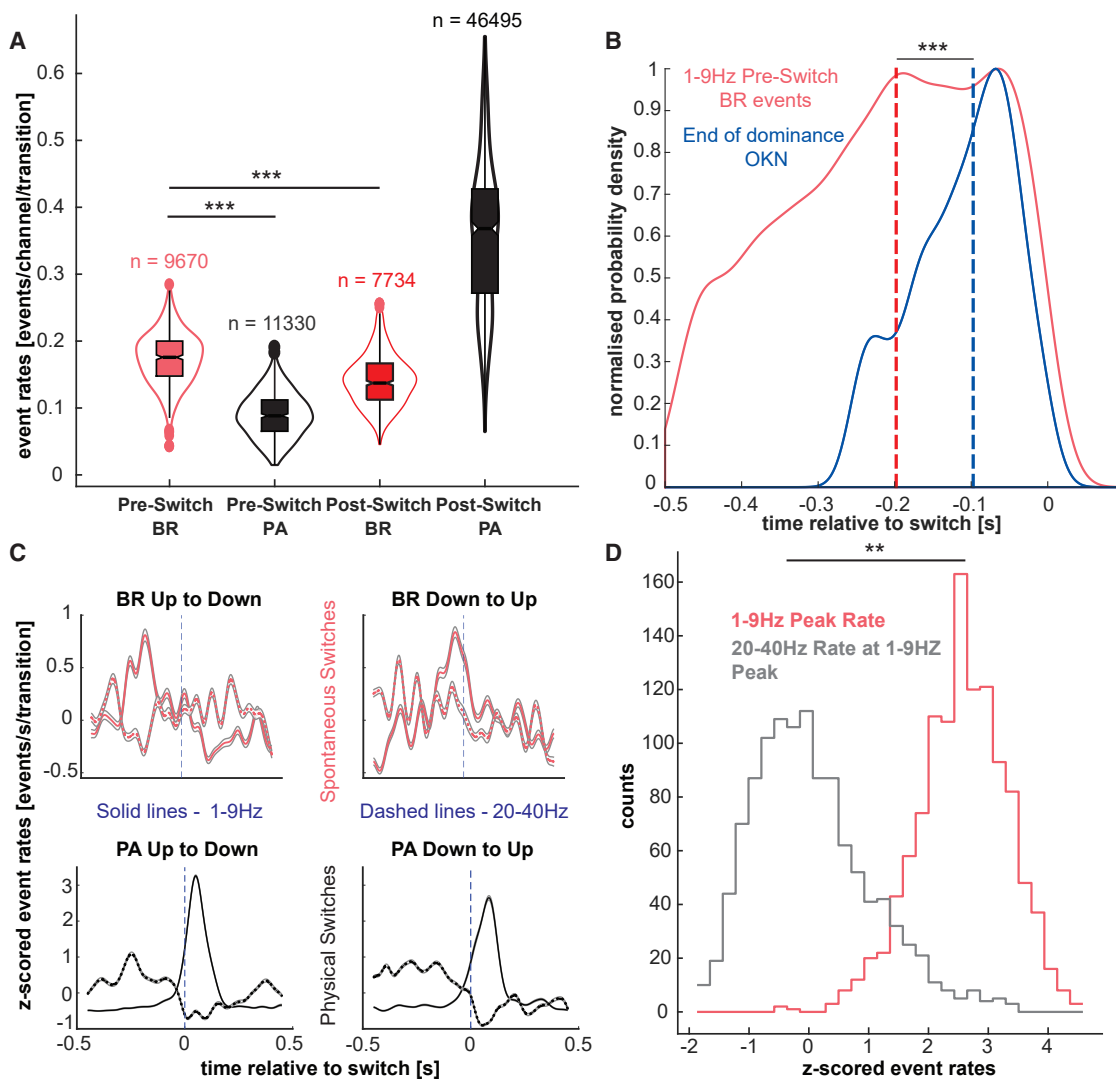


Figure 4. LFP event-rate analysis

(A) Burst rate per transition per channel before and after transitions in PA (red) and BR (black). In order from left to right: pre-BR (dark pink), pre-PA (black), post-BR (light pink), post-PA (gray). Matching color dots represent outliers. More LF events occur before spontaneous but after physical switches. Burst rate before a physical switch is low, suggesting noise levels.

(B) Normalized kernel density estimate of LF event and OKN times marking the end of the previous dominance period. LF events on average occurred before a switch (red dashed line), and significantly before the end of dominance.

(C) Z-scored event rate in time (events/s/transition) during BR (red lines) and PA trials (white lines) for LF (solid lines) and beta activity (dashed lines).

(D) Distribution of beta-band rate (gray) at the peak of LF rate (pink) before spontaneous perceptual transitions in BR showing antagonistic coupling.

$(0.17 \pm 0.0016, n = 9,670, \text{pre-BR} \text{ vs. } 0.14 \pm 0.004, \text{pre-PM}, n = 2,486; p < 10^{-26})$ (Figure 6C), with the LF peak rate occurring after the transition to PM (Figure 6D). Moreover, the event rate was significantly higher after the transition in PM periods ($0.16 \pm 0.004, \text{PM}, n = 3,531 \text{ vs. } 0.14 \pm 0.004, \text{pre-PM}, n = 2,486, \text{events/transition/channel}; p < 10^{-5}$), while the anti-correlation between LF and beta was significant but weaker, compared with clear spontaneous transitions ($r = -0.009, p < 10^{-137} \text{ vs. } r = -0.05; p < 10^{-295}, p < 10^{-14}$; Figures 4D and 6F), suggesting that the strength of LF and beta antagonism is critical for completing a perceptual transition to another period of clear dominance.

Next, we sought to ascertain if there is a difference between LF activity leading to a perceptual transition as compared with LF activity when perceptual transitions do not occur, i.e., during periods of sustained dominance. To accomplish this, we collected LFP activity around randomly triggered time points during these periods. Subtracting the time frequency decomposition of these sustained dominance periods from that of BR preserved the pattern observed in the latter (Figure 6B, compare with BR in Figure 2C). This indicates that weak LF activity occurs as baseline noise, which only leads to a perceptual change when it is spatiotemporally ramped up in a structured manner (Figure 6F vs. Figures 2A and 4C). Indeed, during

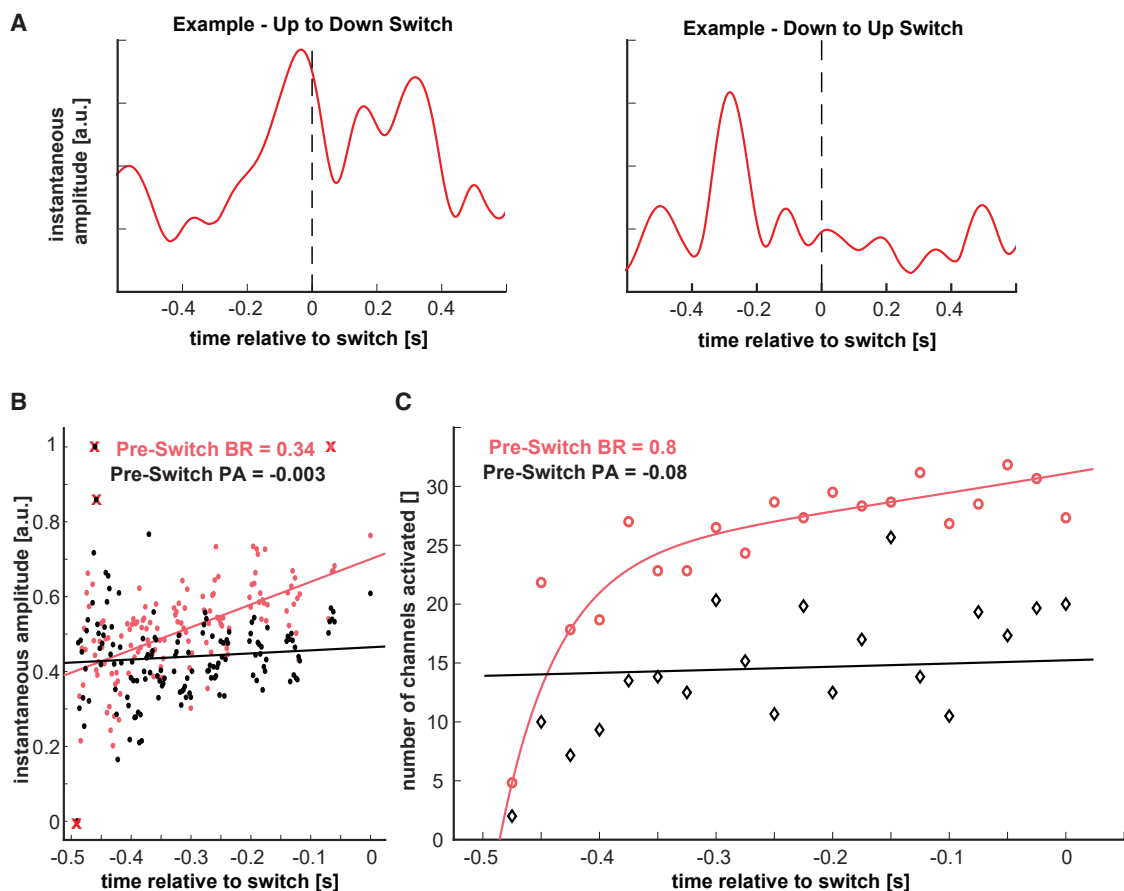


Figure 5. Spatiotemporal buildup preceding spontaneous transitions

(A) Examples of the two types of rivalrous transitions, viz. up to down and down to up, showing a steady increase in LF instantaneous power preceding a switch. (B) Average buildup of LF activity in time. While before BR switch, LF activity ramps up in time (slope = 0.61, $R^2 = 0.34$), before a physical transition, it remains flat (slope = 0.08, $R^2 = -0.003$). X denotes outliers omitted from fitting. (C) The spatiotemporal spread of LF activity manifests in increasing number of prefrontal sites approaching a BR switch, but not a PA switch.

periods of sustained dominance we computed a mean LF event rate of 0.015 ± 0.0005 ($n = 55,026$ after resampling 100 times, i.e., only 550.26 events per iteration) events per sustained dominance period, an order of magnitude lower than the corresponding periods during BR (0.17 ± 0.0016 , $n = 9,670$, Figure 6C). Furthermore, the proportion of sites that displayed LF events approaching all BR switches was 100%, compared with only 51% during sustained dominance where nearly half the recorded sites were silent. These results further indicate that an increase in LF event rate, buildup, and a larger spatial spread of LF activation characterize spontaneous perceptual transitions. Specifically, LF activity should be significantly up modulated from noise level, potentially crossing both a power and spatial spread threshold, to induce a perceptual transition.

Content-specific modulation of global LFP states

Neuronal ensembles selective for the opposing directions of motion in the PFC show a distinct pattern in their firing during BR, where the firing rate follows the dominant or suppressed

direction of motion, depending on the preference of the ensemble (Figure 7A).⁹ However, LF LFPs collected from the electrodes that detected these ensembles do not show such a divergent pattern (Figure 7A). We confirmed this non-selectivity of the LF LFPs by using a support vector machine to decode representations of conscious contents (Figures 7B and S4). Conscious contents could be decoded from population spiking activity but not from LF or beta LFP activity. Therefore, prefrontal LFPs are content-agnostic signals reflecting fluctuations that are not coding for a particular rivaling stimulus. We also fit a piecewise linear function to the spiking activity of every transition with two degrees of freedom in order to detect change points that could point to the start of the change in encoding. This occurs at around -220 ± 10 ms median \pm SD before 0 and significantly after the rise (significantly after the start of rise in peak-rate and event-rate metric, Figures 4C and 7B; correlation data not shown) in LF activity (Figure 7A bottom row dashed line vs. Figure 7B red and pink distributions), confirming the decoupling of content-specific information from the LFPs.

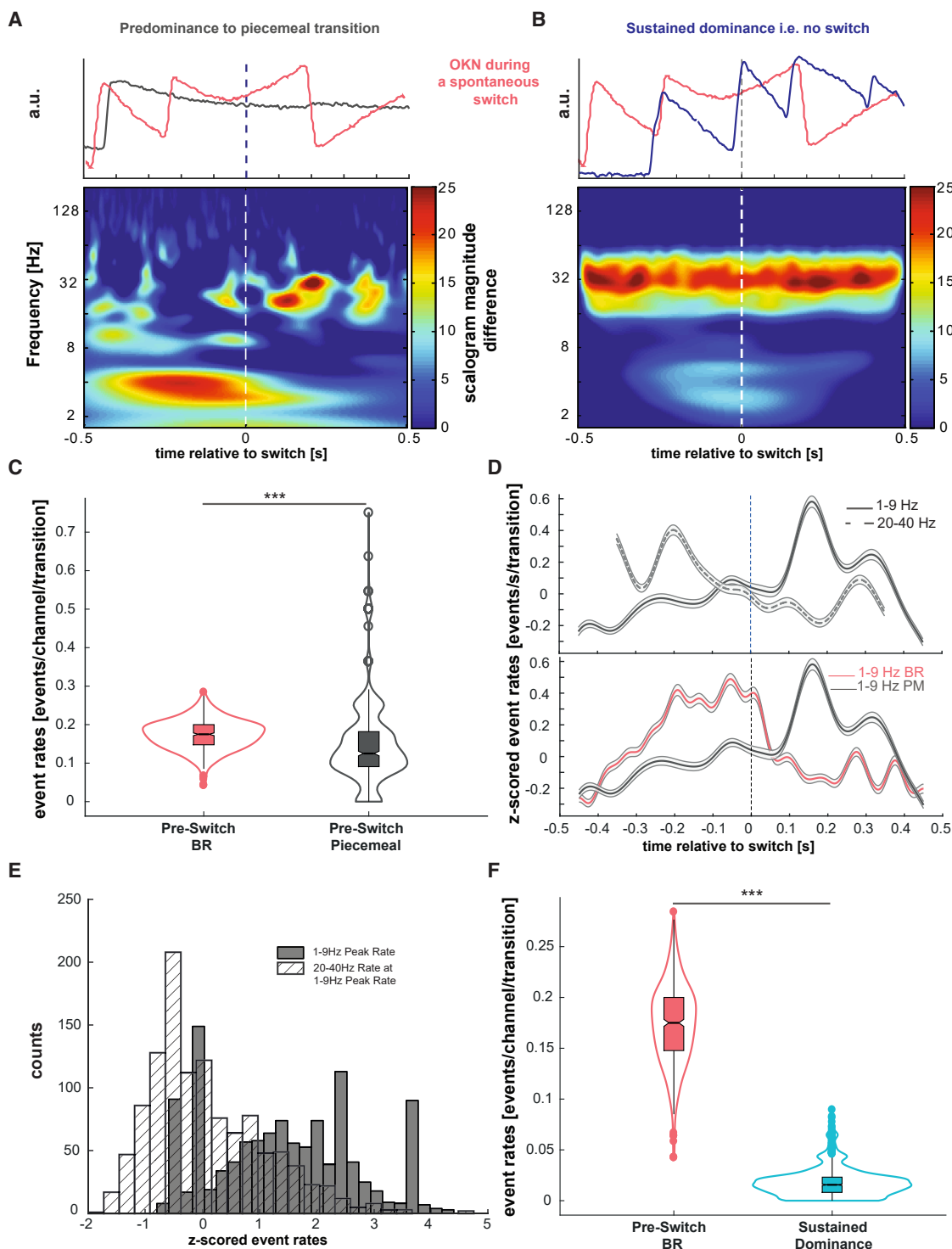


Figure 6. LF amplitude and event rate is critical for inducing clear switches

(A) Top panel: two typical OKN patterns elicited during a spontaneous transition (red) and during a transition to piecemeal (gray). The subtracted spectrogram (BR-PM) below shows a large difference in LF activity before a spontaneous switch, suggesting very weak LF activation before a failed switch.

(B) Top panel shows two typical OKN patterns: spontaneous transition (red) and sustained dominance, i.e., no switches (blue). The subtracted spectrogram preserves the pattern seen before BR, suggesting that LF activity during sustained dominance is minimal.

(C) LF event rate (per transition per channel) before BR is significantly higher than before transition to PM.

(legend continued on next page)

We also investigated whether the non-selective LF LFP activity precedes the change in the encoding of the active conscious percept from the spiking activity of neuronal populations. To understand this temporal relationship, we compared the convergence times of the normalized discharge activity of simultaneously recorded ensembles selective for the rivaling gratings (i.e., the point at which the stimulus-correlated firing rate of the ensembles selective to the dominant and suppressed stimuli flips and reaches saturation, providing a stable ongoing representation of the stimulus) (Figures 7B and S5; see STAR Methods) with the LF event- and peak-rate distributions. Relative to the OKN change signaling a BR switch, we found that discharge activity converged significantly later, compared with both the LF peak rates (-60 ± 222 ms for LFP event/s/transition vs. 209 ± 295 ms, convergence of spiking; $p < 10^{-47}$) and event times (-114 ± 190 ms median event time vs. 209 ± 295 ms, convergence of spiking; $p < 10^{-94}$). In the majority of spontaneous transitions, spiking activity crossovers occurred after the median truncated LF peak rates and event times (in 86.2% of trials compared with peak rates and in 89% of trials compared with event times). These results suggest that LF events, which do not provide an explicit representation of the current conscious content, reflect a pre-conscious process that precedes perceptual update.

To understand how prefrontal state fluctuations relate to spiking-network reorganization and therefore perceptual update and stability, we first plotted the spiking rasters of each transition overlaid with the LF instantaneous power (Figure S6) and the spiking rasters of each negative transient aligned to its trough. Qualitatively, no specific pattern of spike occurrence aligned to the LF power peaks or the negative transients were seen (Figures S6, S7, and S9). However, aligned to negative events detected in both non-preferred to preferred (NP to P) and preferred to non-preferred (P to NP) switch types, a significant increase in population firing rate is observed around the time of the event (Figures S7 and S8), with no significant differences at the peak between the two conditions. Furthermore, in both types of transitions, negative events increased approaching a spontaneous reversal, but the positive events did not (Figure 7C). Therefore, the negative deflections appear to be the most relevant signal that precedes spontaneous perceptual changes, irrespective of the ensemble from which the events are detected, viz. suppressed or dominant.

Because no differences between this activity in competing ensembles could be observed, and because of the quasi-periodic nature of the 1–9 Hz band (and its strong event correlation to observed negative deviations [Figures 2A and 3B]), we hypothesized that differential spike-locking to the ongoing LFP phase could result in spiking network reorganization, leading to crossovers in the observed switch-triggered PSTHs. We therefore performed spike-field coherence⁵⁶ (SFC) and pairwise phase consistency⁵⁷ (PPC) analysis for these competing populations. We computed the SFC in a 1 s window (cut off at 0.9 s to account for edge artifacts) preceding and succeeding a perceptual

switch of the simultaneously recorded, feature-selective ensemble activity and the global broadband LFP across all transitions. After a spontaneous perceptual transition in BR, when the negative LFP deflections and therefore the LF transients were less prevalent, the perceptually dominant ensemble was more coherent in the beta range (~25–37 Hz), compared with the suppressed ensemble (Figures 7D [top and bottom rows] and 7E; $p < 0.03$). However, there were no differences between the suppressed and dominant populations in the period approaching a spontaneous transition when LF transients accompany a suppression of beta bursts. These results suggest that the prefrontal ensemble signaling the current content of consciousness is synchronized in the beta band of the LFP. LF transients dissolve the beta-coherent ensemble, potentially increasing the likelihood for perceptual reorganization. Further evidence for this hypothesis is seen in the mean phase angles of spike-LFP coupling in the LF band (Figure 7F). Before a switch, sites that prefer the suppressed stimulus (i.e., NP to P switch) are locked to the depolarizing phase of the LFP (169.2°), while sites that prefer the dominant stimulus (i.e., P to NP switch) are locked to the hyperpolarizing phase (~147.6°, starting at ~750 ms before the switch, Figure 7F). Although inferring a mechanism from extracellular recordings is challenging, this selective locking could relate to the modulation of the membrane potential, thereby pushing the two ensembles closer to or farther away from the firing threshold, thus increasing or decreasing the firing probability, respectively.

Intrinsic nature of prefrontal state fluctuations

If the competition between LF and beta events that regulate access to visual consciousness is intrinsically generated, reflecting waking state fluctuations, traces of this process should also be observed during resting state—in the absence of any sensory (i.e., visual) input. Indeed, in resting state, LF events suppressed beta activity (Figure 8A). Periods of uninterrupted beta activity, cut off at 10 s to allow for a direct comparison with the psychophysical sample set (Figure 1C), exhibited a gamma distribution with a duration of 1.2 ± 1.44 s, which is close to the psychophysical distribution of stable perceptual dominance durations (1.54 ± 1.28 s) (Figure 8B). However, the full sample set showed a gamma distribution similar to the timescales observed in human bistable studies (data not shown). Therefore, prefrontal state fluctuations appear to reflect an intrinsic process critical to the maintenance and update of conscious information.

DISCUSSION

Our findings suggest that both spontaneous transitions in the content of conscious perception during BR and spontaneous ignitions of content-specific neuronal representations in the PFC are preceded by global (i.e., content-agnostic) LFP state fluctuations. Despite their global nature, these fluctuations are differentially coupled to neuronal populations on a local level. This

(D) Top row: before a transition to PM, beta activity dominates, still signaling the active percept. After the switch, LF inhibits beta, but weakly. Bottom row: LF rate peaks before transition to BR, but after a switch PM.

(E) Distribution of peak LF rates and rate of beta activity at LF peak reveal no significant antagonism before PM, compared with before BR.

(F) LF event rate before a BR switch is significantly higher than during sustained dominance.

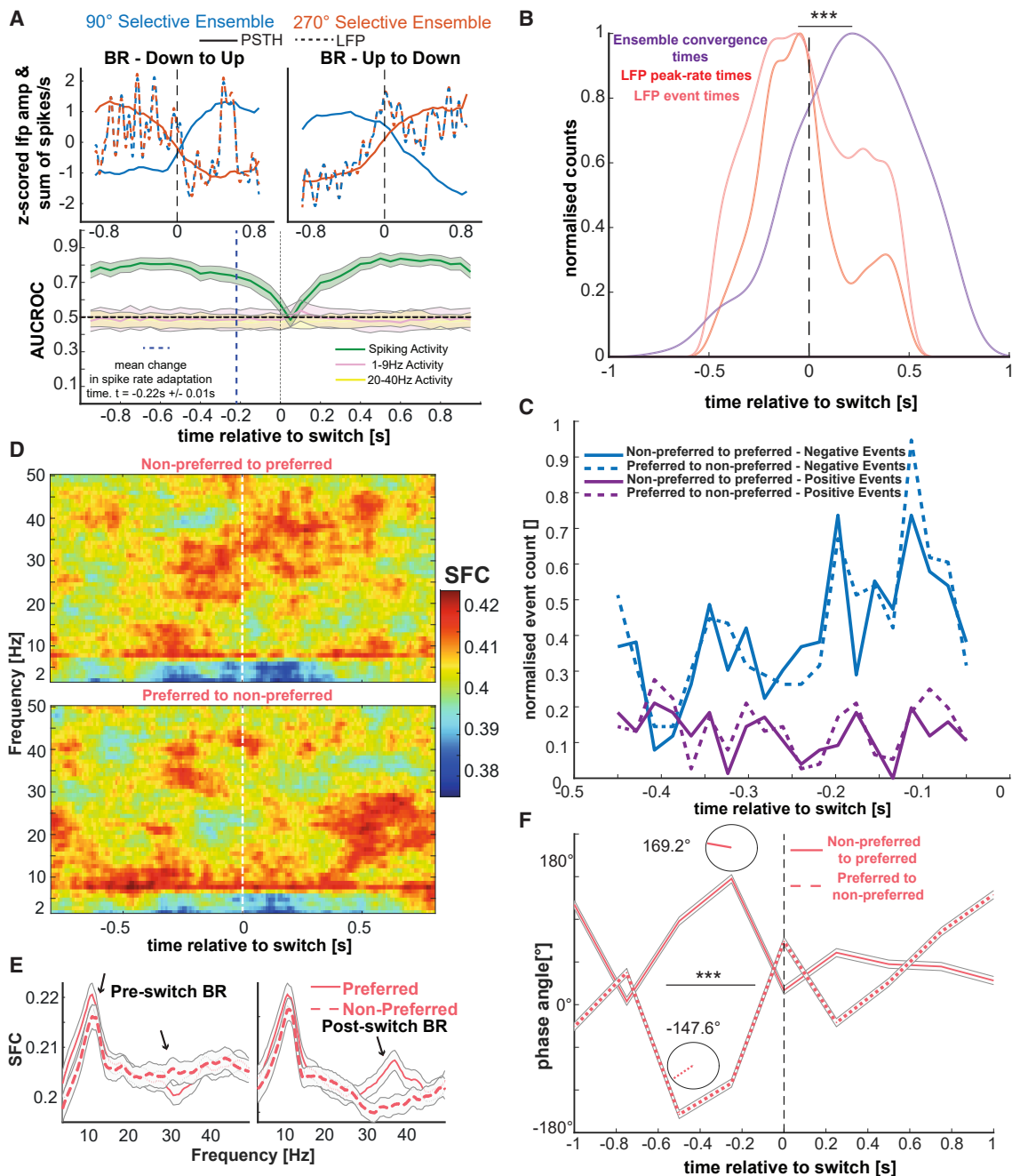


Figure 7. Relationship between the spiking activity of selective ensembles and the LFP

(A) Top row: average population PSTHs of feature-specific neuronal ensembles during BR, showing divergence due to differential encoding, and LF activity, showing no dichotomy. Bottom row: ensemble selectivity (i.e., the content) can be decoded from population spiking, but not from LF or beta-band activity.

(B) Distribution of LF event times (pink), peak-rate times (red), and convergence of PSTHs of competing ensembles (black line) demonstrates that the change in encoding of the conscious content follows LF activity.

(C) Irrespective of the type of switch, i.e., the active ensemble, the number of negative events increases approaching a switch, but the number of positive events remains flat, pointing to the non-specific nature of LF activity.

(D) Top and bottom rows: time-frequency (top) and time-collapsed representation of the spike-field coherence, for non-preferred to preferred (NP to P) and preferred to non-preferred (P to NP) switches, shows the dissolution of beta coherence and its reformation, depending on the switch type.

(E) After a spontaneous transition, spiking of the dominant population was significantly more coherent with the beta LFP band, as compared with the suppressed population (black arrows show significant bins). SFC during pre-switch BR periods, when LF transient events are more prevalent, did not exhibit similar

(legend continued on next page)

coupling depends on whether neuronal populations are in an active state, signaling that their preferred stimulus is consciously perceived, or in an inactive state, signaling that their preferred stimulus is perceptually suppressed. Apart from indicating the role of internal state changes in conscious perception, these results suggest that prefrontal activity is not merely a post-perceptual consequence of conscious perception.^{58,59} Rather, prefrontal LFP state fluctuations precede spontaneous perceptual changes and coding of conscious content from neuronal ensembles in the same area. We discuss these findings in the context of the ongoing debate about the role of PFC in conscious perception, the role of internal state fluctuations in perception and consciousness, and the mechanism of spontaneous transitions in perception during BR.

PFC as part of the cortical network mediating conscious perception

The cortical organization of conscious perception, and in particular the role of PFC, is a topic of controversy since it differentiates theories of consciousness like the GNWT and integrated information theory (IIT).⁶⁰ Previous electrophysiological studies in the PFC have revealed representations of the content of consciousness^{10,34,61,62} as well as preparatory spiking activity before spontaneous perceptual changes.^{61,62} However, these activations could not be dissociated from signals related to voluntary motor reports that were used to indicate perceptual changes. Therefore, it has been suggested that conscious perception emerges in posterior cortical areas, and activity found to correlate with the contents of consciousness in the PFC may reflect only the post-perceptual consequences of conscious perception like correlates of reporting the percept or thinking about the stimulus.^{63–69}

However, our previous neuronal recordings in the NHP PFC suggest that conscious content representations can be decoded with very high accuracy from prefrontal populations, even in the absence of subjective reports.^{9,10,35,70} More recently, multivariate searchlight pattern analysis of fMRI recordings has also demonstrated decoding of conscious contents in frontal areas in both report⁷¹ and no-report conditions.⁷² If conscious contents can be decoded in the PFC, suggesting that PFC is part of a cortical network that represents conscious perception, what is the process that gates the ignition of these representations in the same area? Although ignition in the PFC and PPC has been suggested from GNW as the critical factor enabling conscious access,^{24,27,41,73} a gating mechanism that modulates ignition relying on spontaneous activity fluctuations could be the prerequisite, enabling factor for conscious perception.^{16,25,34,74}

Global state fluctuations precede spontaneous transitions in the content of consciousness

Recent work suggests that cortical state fluctuations during wakefulness are not just noise but rather reflect ongoing fluctu-

ations in attention or arousal states,^{16,19} with the PFC being a critical node for both.^{75–77} Here, we hypothesized that such waking state fluctuations detected in the prefrontal LFP activity could be involved in the spontaneous transitions in the contents of consciousness, which are characterized by ignitions of their neuronal representations in the PFC. We used a no-report BR paradigm, where spontaneous changes in the content of visual consciousness are inferred from spontaneous changes in reflexive eye movements (i.e., OKN). In doing so, we removed any confounds that could be the consequence of post-perceptual processes like voluntary motor reports. Our results suggest that dynamic changes in the prefrontal LFP activity precede spontaneous changes in conscious perception in the absence of voluntary report requirements. Specifically, an increase in LF (1–9 Hz) and a decrease in beta (20–40 Hz) LFP activity occur in the PFC before a spontaneous change in the OKN pattern, known to correlate with the perceived direction of motion.^{49–53} Using a decoding approach, we find that neither LF nor beta LFP amplitude represents the conscious contents but rather reflects content-agnostic fluctuations, which occur before a change in the OKN pattern and before the spontaneous ignition of conscious content representations, decoded from the spiking activity of neuronal populations in the PFC. Crucially, these fluctuations in cortical state are more prevalent in spontaneous transitions from one clear percept (i.e., direction of motion) to the other, compared with transitions from one direction of motion to a PM percept (as inferred from the OKN signal).

Global state fluctuations are locally modulated during conscious perception

Both LF and beta activity were not conveying information about the content of consciousness and were therefore reflecting global state changes that are not stimulus selective. Although pre-stimulus, non-selective, spontaneous fluctuations have been previously shown to influence visual perception of ambiguous stimuli or stimuli presented at threshold,^{74,78–83} it is unclear if and how such global state changes can influence spontaneous transitions of conscious perception between rivaling stimuli in a selective, content-specific manner. Recent theoretical studies have used a content-agnostic signal that related to vigilance, which amplifies neuronal responses homogeneously to explain widespread ignition of neural activity relating to conscious perception for individual stimuli presented at threshold.⁸⁴ However, a content-selective modulation may be critical when neuronal representations compete for conscious access like in BR. Recently, there is indeed evidence that global cortical states can be controlled or modulated locally during spatial attention.^{85,86} Our findings point to a similar fine-scale modulation of global LFP state fluctuations during BR. While fluctuations in the prefrontal state were content agnostic since it was not possible to decode the content of consciousness from the amplitude of the LF and beta LFPs, these two states

differences in the beta band. These effects in the beta band were absent in physical transitions where SFC for a dominant preferred stimulus was significantly reduced in a lower-frequency range.

(F) Mean angles of spike-LFP phase locking during an NP to P (dashed line) and P to NP (solid line) transition. The populations selective to the suppressed stimulus before a switch progressively become locked to the depolarizing phase of the LF LFP (169.2°), thereby causing them to increase their firing rate when their preferred stimulus becomes dominant after the perceptual transition.

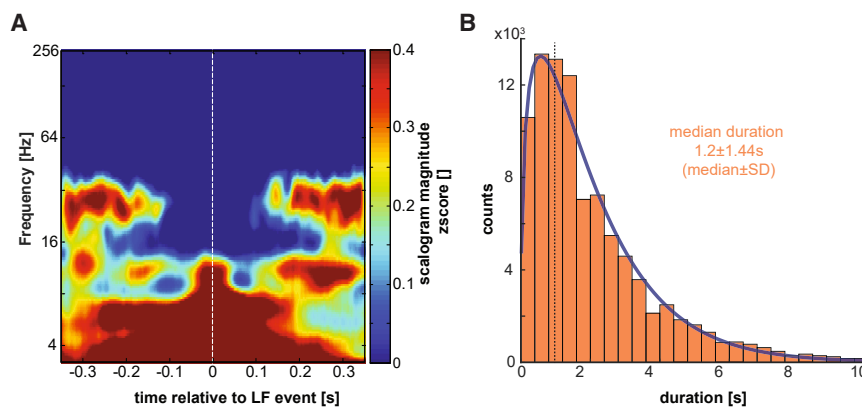


Figure 8. Intrinsic states during resting state show dynamics similar to perceptual transitions

(A) Grand-average ($n = 480$), LF event-triggered spectrogram during resting state showing cortical state fluctuations between LF and beta activity in the absence of structured sensory input.
(B) Periods of sustained beta activation during resting state. The median duration is remarkably similar to the psychophysical gamma distribution (Figure 1C).

interacted differentially with the competing neuronal populations. Specifically, global fluctuations were found to be dynamically modulated on a local level since (1) conscious and non-conscious neuronal representations were locked differentially to the phase of LF activity just before a spontaneous perceptual transition and (2) neuronal populations were coherent with beta activity only when their preferred stimulus was perceptually dominant (i.e., consciously perceived) during BR. These results, pointing to the existence of both global state fluctuations and their local modulation influencing conscious perception during BR in a mesoscopic scale, are in agreement with recent MEG studies showing evidence for both a general pre-stimulus process that is agnostic for the stimulus category and a specific pre-stimulus process that facilitates category-specific recognition.⁷⁴

Beta LFP state reflects perceptual stability during BR

What is the role of beta bursts in the PFC during BR? Beta activity has been suggested to reflect an intrinsic mode of cortical operation that shields ongoing behavioral and cognitive or sensory processing states (status quo) from interference and distractors.^{87–89} As a consequence, transient decreases in cortical beta activity could increase sensory information relay,^{4,11,90–93} providing a mechanism for controlling bottom-up sensory processing through top-down knowledge⁹² that can be content specific.⁹¹

Our findings are in agreement with such a role for beta activity during BR. Beta activity was prominent during periods of perceptual stability, in agreement with scalp EEG and MEG recordings.^{94,95} In particular, neuronal populations were coherently firing in the beta range when their preferred direction of motion was perceived. Dissolution of these content-specific, beta-coherent ensembles from low-frequency activity occurred before spontaneously generated changes in the OKN, signaling perceptual updates. Therefore, beta and LF LFP activity compete in the PFC, reflecting a competition between perceptual stability and updates, respectively. This result is also reminiscent of content (i.e., rule)-selective prefrontal ensembles that are coherent in the beta band with LF activity inhibiting a rule that is about to be deselected.^{96,97} This suggests that conscious perception and cognitive control might recruit similar processes in the PFC.

Prefrontal state fluctuations and gating of access to consciousness

We suggest that these findings could reflect a gating-like mechanism,^{46,98,99} where intrinsically generated fluctuations in the prefrontal cortical state between periods of LF and beta events gate the access of competing perceptual representations to consciousness. Specifically, the disruption of intrinsically generated beta activity by LF activity could reflect the process (perhaps related to fluctuations in arousal or attention) that controls the prefrontal ignition mechanism that has long been hypothesized to gate or control access to consciousness.^{34,73,100–102}

Importantly, we show here that the LF activation occurs earlier compared with both the spontaneous changes in OKN, which are used to infer spontaneous perceptual changes, and the activity of content-selective ensembles. Therefore, it appears that the driver of perceptual reorganization and update might not be the spiking activity of selective neuronal ensembles (which however do show fluctuations before a spontaneous transition); rather, it is a global state signal. Interestingly, during competition between two content representations in BR, these global fluctuations are modulated locally, providing a potential mechanism for content-specific spontaneous changes in conscious perception. This top-down mechanism of perceptual reorganization that has been proposed to drive multistable perception¹³ is fundamentally different from bottom-up mechanisms, proposing that competition between monocular neurons in the V1 resolves BR.^{13,26} Neuronal activity in V1 is indeed only weakly modulated during BR in both monocular and binocular neurons,¹³ while BOLD modulation of V1 is detected in superficial layers, suggesting feedback from higher cortical areas.¹⁰³ Furthermore, ocular dominance columns in V1 rival even during anesthesia,³¹ indicating that V1 activity is not alone sufficient for conscious visual perception.

Limitations of the study

We recorded neural activity only in the PFC and not in other cortical regions. It is therefore unclear whether the prefrontal state change preceding spontaneous transitions is an isolated PFC phenomenon or whether it can be observed or originates in other regions. For example, the anterior insula was recently shown using fMRI to have a gating role in conscious perception by regulating transitions between the default mode and dorsal

attention network.¹⁰⁴ Furthermore, whether the LFP state change before spontaneous perceptual transitions is also observed in the PPC (part of the frontoparietal loop in GNW) is unknown. Multi-site recordings during paradigms of conscious visual perception may help to address the spatial extent and source of these internal state fluctuations.

Another limitation of our study is the difficulty in establishing a firm causal relationship between global changes in the LFP signal and spiking activity, in particular between the LF activity increase and the adaptation in spiking activity that both seem to occur before a spontaneous perceptual transition. The co-occurrence of these processes might indicate that both contribute to a spontaneous perceptual switch. Indeed, theoretical studies have shown that spontaneous changes in BR can be explained as the interplay between deterministic (adaptation and inhibition) and stochastic (noise) forces. In these models, adaptation acts to reduce the inhibition between two pools of neurons that compete for perceptual dominance^{26,105} up to a point where noise drives the transitions.^{106–108} Specifically, adaptation acts to reduce the energy required to transition from one (neuronal) well to another. It is possible that our results reflect these dynamics with both adaptation in encoding and internal noise (i.e., spontaneous LFP state fluctuations) inducing the final transition. We should note, however, that noise (which might relate to internal state fluctuations) is the critical factor in these models since adaptation alone cannot explain the temporal dynamics during BR.

Finally, our study explains the findings based on the GNWT, where conscious perception relates to access consciousness that is characterized by ignition of neural activity and sensory information being broadcasted in a wide cortical network that includes the frontoparietal network.^{24,27} By contrast, IIT suggests that consciousness has a shorter timescale,¹⁰⁹ relies more on posterior cortical areas,⁶⁵ and is characterized by phenomenal experience.¹¹⁰ Despite these theoretical differences, visual stimuli can be decoded from early (~50 ms) neuronal activity in both the PFC and PPC, even under rapid serial visual presentation conditions that might weaken conscious access, suggesting that phenomenal consciousness may also be detected in areas assumed to be involved only in access consciousness.³⁵ Although beyond the scope of this study, the influence of prefrontal state fluctuations in phenomenal vs. access consciousness, and more generally in the predictions of different theories of consciousness, could be a promising field of future investigation.

Conclusions

Spontaneous cortical activity can attain various states during wakefulness that reflect variations in arousal and attention states, replay of sensory-driven activity, or multi-dimensional representations of behaviors and context.^{16,111,112} In the PFC, we observed a suppression of ongoing beta events during LF transients that precedes spontaneous changes in conscious perception. The same pattern was also observed during periods of resting state. This suggests that the source of spontaneous transitions in the content of consciousness may be the interaction of visual input representations with ongoing, waking state fluctuations. Taken together, our results reveal a potential role of prefrontal state fluctuations in a gating process that mediates the emergence of conscious perception.

STAR METHODS

Detailed methods are provided in the online version of this paper and include the following:

- KEY RESOURCES TABLE
- RESOURCE AVAILABILITY
 - Lead contact
 - Materials availability
 - Data and code availability
- EXPERIMENTAL MODEL AND SUBJECT DETAILS
- METHOD DETAILS
 - Electrophysiological recordings
 - Data acquisition, spike sorting and local field potentials
 - Visual stimulation and experimental paradigm
 - Detection of spontaneous transitions
 - Treatment of the LFP data
 - Construction of direction of motion specific neural ensembles
 - Spike-field Coherence
 - Treatment of resting-state activity
 - Statistical analysis

SUPPLEMENTAL INFORMATION

Supplemental information can be found online at <https://doi.org/10.1016/j.neuron.2023.02.027>.

ACKNOWLEDGMENTS

We thank Dr. Yusuke Murayama and the other technical and animal care staff of the MPI for Biological Cybernetics for excellent technical assistance, Prof. Dr. Nicho Hatsopoulos for help with the implantations of the Utah arrays, Prof. Dr. Stanislas Dehaene for his inputs and insights, and Mr. Akshat Jain for his assistance in the preparation of publishable quality figures. We would also like to thank Dr. Michel Besserve, Prof. Dr. B.S. Dwarakanath, and Dr. Majid Khalili-Ardali for helpful discussions and comments in a previous version of the manuscript. The Max Planck Society supported this study. The Templeton World Charity Foundation, Inc. (TWCF0562) currently supports T.I.P. N.K.L. and V.K. presently receive funding through the Shanghai Municipal Science and Technology Major Project (grant no. 2019SHZDZX02).

AUTHOR CONTRIBUTIONS

Conceptualization, A.D., V.K., N.K.L., and T.I.P. (lead); data curation, A.D. (lead), V.K., and J.W.; formal analysis, A.D. (lead), V.K., J.W., and L.A.F.; funding acquisition, N.K.L.; investigation, A.D. (equal), V.K. (equal), and T.I.P. (supporting); methodology, A.D. (equal), V.K. (equal), J.W. (supporting), S.S. (supporting), and T.I.P. (equal); project administration, T.I.P.; resources, J.W. and N.K.L. (lead); software, A.D. (lead), V.K., J.W., L.A.F., and S.S. (supporting); supervision, T.I.P.; visualization, A.D. (lead) and T.I.P. (supporting); writing – original draft, A.D. and T.I.P. (lead); writing – review & editing, A.D., V.K., L.A.F., S.S., N.K.L., and T.I.P. (lead).

DECLARATION OF INTERESTS

The authors declare no competing interests.

Received: June 10, 2022

Revised: October 24, 2022

Accepted: February 16, 2023

Published: March 14, 2023

REFERENCES

1. Leopold, D.A., and Logothetis, N.K. (1999). Multistable phenomena: changing views in perception. *Trends Cogn.Sci.* 3, 254–264. [https://doi.org/10.1016/s1364-6613\(99\)01332-7](https://doi.org/10.1016/s1364-6613(99)01332-7).
2. Seth, A.K., and Bayne, T. (2022). Theories of consciousness. *Nat. Rev. Neurosci.* 23, 439–452. <https://doi.org/10.1038/s41583-022-00587-4>.
3. Blake, R., Brascamp, J., and Heeger, D.J. (2014). Can binocular rivalry reveal neural correlates of consciousness? *Philos. Trans. R. Soc. Lond. B Biol. Sci.* 369, 20130211. <https://doi.org/10.1098/rstb.2013.0211>.
4. Maier, A., Panagiotaropoulos, T.I., Tsuchiya, N., and Keliris, G.A. (2012). Introduction to research topic - binocular rivalry: a gateway to studying consciousness. *Front. Hum. Neurosci.* 6, 263. <https://doi.org/10.3389/fnhum.2012.00263>.
5. Logothetis, N.K. (1998). Single units and conscious vision. *Philos. Trans. R. Soc. Lond. B Biol. Sci.* 353, 1801–1818. <https://doi.org/10.1098/rstb.1998.0333>.
6. Blake, R., and Logothetis, N.K. (2002). Visual competition. *Nat. Rev. Neurosci.* 3, 13–21. <https://doi.org/10.1038/nrn701>.
7. Clifford, C.W.G. (2009). Binocular rivalry. *Curr. Biol.* 19, R1022–R1023. <https://doi.org/10.1016/j.cub.2009.09.006>.
8. Blake, R. (2001). A primer on binocularrivalry, includingcurrentcontroversies. *BrainMind* 2, 5–38.
9. Kapoor, V., Dwarakanath, A., Safavi, S., Werner, J., Besserve, M., Panagiotaropoulos, T.I., and Logothetis, N.K. (2022). Decoding internally generated transitions of conscious contents in the prefrontal cortex without subjective reports. *Nat. Commun.* 13, 1535. <https://doi.org/10.1038/s41467-022-28897-2>.
10. Panagiotaropoulos, T.I., Deco, G., Kapoor, V., and Logothetis, N.K. (2012). Neuronal discharges and gamma oscillations explicitly reflect visual consciousness in the lateral prefrontal cortex. *Neuron* 74, 924–935. <https://doi.org/10.1016/j.neuron.2012.04.013>.
11. Panagiotaropoulos, T.I., Kapoor, V., and Logothetis, N.K. (2014). Subjective visual perception: from local processing to emergent phenomena of brain activity. *Philos. Trans. R. Soc. Lond. B Biol. Sci.* 369, 20130534. <https://doi.org/10.1098/rstb.2013.0534>.
12. Sheinberg, D.L., and Logothetis, N.K. (1997). The role of temporal cortical areas in perceptual organization. *Proc.Natl.Acad.Sci. USA* 94, 3408–3413. <https://doi.org/10.1073/pnas.94.7.3408>.
13. Leopold, D.A., and Logothetis, N.K. (1996). Activity changes in early visual cortex reflect monkeys' percepts during binocular rivalry. *Nature* 379, 549–553. <https://doi.org/10.1038/379549a0>.
14. Logothetis, N.K., and Schall, J.D. (1989). Neuronal correlates of subjective visual perception. *Science* 245, 761–763. <https://doi.org/10.1126/science.2772635>.
15. Sterzer, P., Kleinschmidt, A., and Rees, G. (2009). The neural bases of multistable perception. *Trends Cogn.Sci.* 13, 310–318. <https://doi.org/10.1016/j.tics.2009.04.006>.
16. McGinley, M.J., Vinck, M., Reimer, J., Batista-Brito, R., Zagha, E., Cadwell, C.R., Tolias, A.S., Cardin, J.A., and McCormick, D.A. (2015). Waking state: rapid variations modulate neural and behavioral responses. *Neuron* 87, 1143–1161. <https://doi.org/10.1016/j.neuron.2015.09.012>.
17. Luczak, A., Barthó, P., and Harris, K.D. (2009). Spontaneous events outline the realm of possible sensory responses in neocortical populations. *Neuron* 62, 413–425. <https://doi.org/10.1016/j.neuron.2009.03.014>.
18. Luczak, A., Barthó, P., and Harris, K.D. (2013). Gating of sensory input by spontaneous cortical activity. *J. Neurosci.* 33, 1684–1695. <https://doi.org/10.1523/JNEUROSCI.2928-12.2013>.
19. Harris, K.D., and Thiele, A. (2011). Cortical state and attention. *Nat. Rev. Neurosci.* 12, 509–523. <https://doi.org/10.1038/nrn3084>.
20. Ringach, D.L. (2009). Spontaneous and driven cortical activity: implications for computation. *Curr. Opin. Neurobiol.* 19, 439–444. <https://doi.org/10.1016/j.conb.2009.07.005>.
21. Avitan, L., and Stringer, C. (2022). Not so spontaneous: multi-dimensional representations of behaviors and context in sensory areas. *Neuron* 110, 3064–3075. <https://doi.org/10.1016/j.neuron.2022.06.019>.
22. Stringer, C., Pachitariu, M., Steinmetz, N., Reddy, C.B., Carandini, M., and Harris, K.D. (2019). Spontaneous behaviors drive multidimensional, brainwide activity. *Science* 364, 255. <https://doi.org/10.1126/science.aav7893>.
23. Fisch, L., Privman, E., Ramot, M., Harel, M., Nir, Y., Kipervasser, S., Andelman, F., Neufeld, M.Y., Kramer, U., Fried, I., and Malach, R. (2009). Neural “ignition”: enhanced activation linked to perceptual awareness in human ventral stream visual cortex. *Neuron* 64, 562–574. <https://doi.org/10.1016/j.neuron.2009.11.001>.
24. Dehaene, S., and Changeux, J.P. (2011). Experimental and theoretical approaches to conscious processing. *Neuron* 70, 200–227. <https://doi.org/10.1016/j.neuron.2011.03.018>.
25. Moutard, C., Dehaene, S., and Malach, R. (2015). Spontaneous fluctuations and non-linear ignitions: twodynamicfaces of corticalrecurrentloops. *Neuron* 88, 194–206. <https://doi.org/10.1016/j.neuron.2015.09.018>.
26. Blake, R. (1989). A neural theory of binocular rivalry. *Psychol. Rev.* 96, 145–167. <https://doi.org/10.1037/0033-295X.96.1.145>.
27. Mashour, G.A., Roelfsema, P., Changeux, J.P., and Dehaene, S. (2020). Conscious processing and the global neuronal workspace hypothesis. *Neuron* 105, 776–798. <https://doi.org/10.1016/j.neuron.2020.01.026>.
28. Dehaene, S., Changeux, J.-P., and Naccache, L. (2011). The global neuronal workspace model of conscious access: from neuronal architectures to clinical applications. In *Characterizing Consciousness: From Cognition to the Clinic? Research and Perspectives in Neurosciences*, S. Dehaene and Y. Christen, eds. (Springer), pp. 55–84. https://doi.org/10.1007/978-3-642-18015-6_4.
29. Metzger, B.A., Mathewson, K.E., Tapia, E., Fabiani, M., Gratton, G., and Beck, D.M. (2017). Regulating the access to awareness: brainactivityrelated to probe-related and spontaneousreversals in binocularrivalry. *J. Cogn. Neurosci.* 29, 1089–1102. https://doi.org/10.1162/jocn_a_01104.
30. Logothetis, N.K., Leopold, D.A., and Sheinberg, D.L. (1996). What is rivalry during binocular rivalry? *Nature* 380, 621–624. <https://doi.org/10.1038/380621a0>.
31. Xu, H., Han, C., Chen, M., Li, P., Zhu, S., Fang, Y., Hu, J., Ma, H., and Lu, H.D. (2016). Rivalry-like neuralactivity in primaryvisualcortex in anesthetizedmonkeys. *J. Neurosci.* 36, 3231–3242. <https://doi.org/10.1523/JNEUROSCI.3660-15.2016>.
32. Zou, J., He, S., and Zhang, P. (2016). Binocular rivalry from invisible patterns. *Proc.Natl.Acad.Sci. USA* 113, 8408–8413. <https://doi.org/10.1073/pnas.1604816113>.
33. Lumer, E.D., Friston, K.J., and Rees, G. (1998). Neural correlates of perceptual rivalry in the human brain. *Science* 280, 1930–1934. <https://doi.org/10.1126/science.280.5371.1930>.
34. van Vugt, B., Dagnino, B., Vartak, D., Safaai, H., Panzeri, S., Dehaene, S., and Roelfsema, P.R. (2018). The threshold for conscious report: signal loss and response bias in visual and frontal cortex. *Science* 360, 537–542. <https://doi.org/10.1126/science.aar7186>.
35. Bellet, J., Gay, M., Dwarakanath, A., Jarraya, B., van Kerkoerle, T., Dehaene, S., and Panagiotaropoulos, T.I. (2022). Decoding rapidly presented visual stimuli from prefrontal ensembles without report nor post-perceptual processing. *Neurosci. Conscious.* 2022, niac005. <https://doi.org/10.1093/nc/niac005>.
36. Levinson, M., Podvalny, E., Baete, S.H., and He, B.J. (2021). Cortical and subcortical signatures of conscious object recognition. *Nat. Commun.* 12, 2930. <https://doi.org/10.1038/s41467-021-23266-x>.
37. Weilhammer, V., Fritsch, M., Chikermane, M., Eckert, A.L., Kanthak, K., Stuke, H., Kaminski, J., and Sterzer, P. (2021). An active role of inferior frontal cortex in conscious experience. *Curr. Biol.* 31, 2868–2880.e8. <https://doi.org/10.1016/j.cub.2021.04.043>.

38. Dehaene, S., and Changeux, J.P. (2005). Ongoing spontaneous activity controls access to consciousness: a neuronal model for inattentional blindness. *PLoS Biol.* 3, e141. <https://doi.org/10.1371/journal.pbio.0030141>.
39. Doesburg, S.M., Green, J.J., McDonald, J.J., and Ward, L.M. (2009). Rhythms of consciousness: binocular rivalry reveals large-scale oscillatory network dynamics mediating visual perception. *PLoS One* 4, e6142. <https://doi.org/10.1371/journal.pone.0006142>.
40. Kang, Y.H.R., Petzschner, F.H., Wolpert, D.M., and Shadlen, M.N. (2017). Piercing of consciousness as a threshold-crossing operation. *Curr. Biol.* 27, 2285–2295.e6. <https://doi.org/10.1016/j.cub.2017.06.047>.
41. Dehaene, S., Naccache, L., Cohen, L., Bihan, D.L., Mangin, J.F., Poline, J.B., and Rivière, D. (2001). Cerebral mechanisms of word masking and unconscious repetition priming. *Nat. Neurosci.* 4, 752–758. <https://doi.org/10.1038/89551>.
42. Noy, N., Bickel, S., Zion-Golumbic, E., Harel, M., Golan, T., Davidesco, I., Schevon, C.A., McKhann, G.M., Goodman, R.R., Schroeder, C.E., et al. (2015). Ignition's glow: ultra-fast spread of global cortical activity accompanying local "ignitions" in visual cortex during conscious visual perception. *Conscious. Cogn.* 35, 206–224. <https://doi.org/10.1016/j.concog.2015.03.006>.
43. Del Cul, A., Baillet, S., and Dehaene, S. (2007). Brain dynamics underlying the nonlinear threshold for access to consciousness. *PLoS Biol.* 5, e260. <https://doi.org/10.1371/journal.pbio.0050260>.
44. Joglekar, M.R., Mejias, J.F., Yang, G.R., and Wang, X.J. (2018). Inter-area balanced amplification enhances signal propagation in a large-scale-circuit model of the primate cortex. *Neuron* 98, 222–234.e8. <https://doi.org/10.1016/j.neuron.2018.02.031>.
45. Noel, J.P., Ishizawa, Y., Patel, S.R., Eskandar, E.N., and Wallace, M.T. (2019). Leveraging nonhuman primate multisensory neurons and circuits in assessing consciousness theory. *J. Neurosci.* 39, 7485–7500. <https://doi.org/10.1523/JNEUROSCI.0934-19.2019>.
46. O'Reilly, R.C. (2006). Biologically based computational models of high-level cognition. *Science* 314, 91–94. <https://doi.org/10.1126/science.1127242>.
47. Petrides, M. (2005). Lateral prefrontal cortex: architectonic and functional organization. *Philos. Trans. R. Soc. Lond. B Biol. Sci.* 360, 781–795. <https://doi.org/10.1098/rstb.2005.1631>.
48. Petrides, M., and Pandya, D.N. (1984). Projections to the frontal cortex from the posterior parietal region in the rhesus monkey. *J. Comp. Neurol.* 228, 105–116. <https://doi.org/10.1002/cne.902280110>.
49. Fox, R., Todd, S., and Bettinger, L.A. (1975). Optokinetic nystagmus as an objective indicator of binocular rivalry. *Vision Res.* 15, 849–853. [https://doi.org/10.1016/0042-6989\(75\)90265-5](https://doi.org/10.1016/0042-6989(75)90265-5).
50. Logothetis, N.K., and Schall, J.D. (1990). Binocular motion rivalry in macaque monkeys: eye dominance and tracking eye movements. *Vision Res.* 30, 1409–1419. [https://doi.org/10.1016/0042-6989\(90\)90022-d](https://doi.org/10.1016/0042-6989(90)90022-d).
51. Naber, M., Frässle, S., and Einhäuser, W. (2011). Perceptual rivalry: reflexes reveal the gradual nature of visual awareness. *PLoS One* 6, e20910. <https://doi.org/10.1371/journal.pone.0020910>.
52. Fujiwara, M., Ding, C., Kaunitz, L., Stout, J.C., Thyagarajan, D., and Tsuchiya, N. (2017). Optokinetic nystagmus reflects perceptual directions in the onset binocular rivalry in Parkinson's disease. *PLoS One* 12, e0173707. <https://doi.org/10.1371/journal.pone.0173707>.
53. Aleshin, S., Ziman, G., Kovács, I., and Braun, J. (2019). Perceptual reversals in binocular rivalry: improved detection from OKN. *J. Vis.* 19, 5. <https://doi.org/10.1167/19.3.5>.
54. Zhou, Y.H., Gao, J.B., White, K.D., Merk, I., and Yao, K. (2004). Perceptual dominance time distributions in multistable visual perception. *Biol. Cybern.* 90, 256–263. <https://doi.org/10.1007/s00422-004-0472-8>.
55. Brascamp, J.W., van Ee, R., Pestman, W.R., and van den Berg, A.V. (2005). Distributions of alternation rates in various forms of bistable perception. *J. Vis.* 5, 287–298. <https://doi.org/10.1167/5.4.1>.
56. Chandrasekaran, C., Trubanova, A., Stillitano, S., Caplier, A., and Ghazanfar, A.A. (2009). The natural statistics of audiovisual speech. *PLoS Comput. Biol.* 5, e1000436. <https://doi.org/10.1371/journal.pcbi.1000436>.
57. van der Meer, M.A.A., and Redish, A.D. (2009). Low and highgamma oscillations in ratventralstriatum have distinctrelationships to behavior, reward, and spikingactivity on a learnedspatialdecisiontask. *Front. Integr. Neurosci.* 3, 9. <https://doi.org/10.3389/neuro.07.009.2009>.
58. Aru, J., Bachmann, T., Singer, W., and Melloni, L. (2012). Distilling the neural correlates of consciousness. *Neurosci. Biobehav. Rev.* 36, 737–746. <https://doi.org/10.1016/j.neubiorev.2011.12.003>.
59. Block, N. (2020). Finessing the bored monkey problem. *Trends Cogn.Sci.* 24, 167–168. <https://doi.org/10.1016/j.tics.2019.12.012>.
60. Melloni, L., Mudrik, L., Pitts, M., and Koch, C. (2021). Making the hard problem of consciousness easier. *Science* 372, 911–912. <https://doi.org/10.1126/science.abj3259>.
61. Gelbard-Sagiv, H., Mudrik, L., Hill, M.R., Koch, C., and Fried, I. (2018). Human single neuron activity precedes emergence of conscious perception. *Nat. Commun.* 9, 2057. <https://doi.org/10.1038/s41467-018-03749-0>.
62. Libedinsky, C., and Livingstone, M. (2011). Role of prefrontal cortex in conscious visual perception. *J. Neurosci.* 31, 64–69. <https://doi.org/10.1523/JNEUROSCI.3620-10.2011>.
63. Boly, M., Massimini, M., Tsuchiya, N., Postle, B.R., Koch, C., and Tononi, G. (2017). Are the neural correlates of consciousness in the front or in the back of the cerebral cortex? clinical and neuroimaging evidence. *J. Neurosci.* 37, 9603–9613. <https://doi.org/10.1523/JNEUROSCI.3218-16.2017>.
64. Frässle, S., Sommer, J., Jansen, A., Naber, M., and Einhäuser, W. (2014). Binocular rivalry: frontal activity relates to introspection and action but not to perception. *J. Neurosci.* 34, 1738–1747. <https://doi.org/10.1523/JNEUROSCI.4403-13.2014>.
65. Koch, C., Massimini, M., Boly, M., and Tononi, G. (2016). Neural correlates of consciousness: progress and problems. *Nat. Rev. Neurosci.* 17, 307–321. <https://doi.org/10.1038/nrn.2016.22>.
66. Tsuchiya, N., Wilke, M., Frässle, S., and Lamme, V.A.F. (2015). No-report-paradigms: extracting the true neuralcorrelates of consciousness. *Trends Cogn.Sci.* 19, 757–770. <https://doi.org/10.1016/j.tics.2015.10.002>.
67. Lamme, V.A.F. (2006). Towards a true neural stance on consciousness. *Trends Cogn.Sci.* 10, 494–501. <https://doi.org/10.1016/j.tics.2006.09.001>.
68. Sandberg, K., Frässle, S., and Pitts, M. (2016). Future directions for identifying the neural correlates of consciousness. *Nat. Rev. Neurosci.* 17, 666. <https://doi.org/10.1038/nrn.2016.104>.
69. Boly, M., Seth, A.K., Wilke, M., Ingmundson, P., Baars, B., Laureys, S., Edelman, D.B., and Tsuchiya, N. (2013). Consciousness in humans and non-human animals: recent advances and future directions. *Front. Psychol.* 4, 625. <https://doi.org/10.3389/fpsyg.2013.00625>.
70. Panagiotaropoulos, T.I., Dwarakanath, A., and Kapoor, V. (2020). Prefrontal cortex and consciousness: beware of the signals. *Trends Cogn.Sci.* 24, 343–344. <https://doi.org/10.1016/j.tics.2020.02.005>.
71. Liu, S., Yu, Q., Tse, P.U., and Cavanagh, P. (2019). Neural correlates of the conscious perception of visual location lie outside visual cortex. *Curr. Biol.* 29, 4036–4044.e4. <https://doi.org/10.1016/j.cub.2019.10.033>.
72. Hatamimajoumerd, E., Ratan Murty, N.A., Pitts, M., and Cohen, M.A. (2022). Decoding perceptual awareness across the brain with a no-report fMRI masking paradigm. *Curr. Biol.* 32, 4139–4149.e4. <https://doi.org/10.1016/j.cub.2022.07.068>.
73. Dehaene, S., and Naccache, L. (2001). Towards a cognitive neuroscience of consciousness: basic evidence and a workspace framework. *Cognition* 79, 1–37. [https://doi.org/10.1016/S0010-0277\(00\)00123-2](https://doi.org/10.1016/S0010-0277(00)00123-2).
74. Podvalny, E., Flounders, M.W., King, L.E., Holroyd, T., and He, B.J. (2019). A dual role of prestimulus spontaneous neural activity in visual object recognition. *Nat. Commun.* 10, 3910. <https://doi.org/10.1038/s41467-019-11877-4>.

75. Martinez-Trujillo, J. (2022). Visual attention in the prefrontal cortex. *Annu. Rev. Vis. Sci.* 8, 407–425. <https://doi.org/10.1146/annurev-vision-100720-031711>.
76. Mashour, G.A., Pal, D., and Brown, E.N. (2022). Prefrontal cortex as a key node in arousal circuitry. *Trends Neurosci.* 45, 722–732. <https://doi.org/10.1016/j.tins.2022.07.002>.
77. Pal, D., and Mashour, G.A. (2022). General anesthesia and the cortical stranglehold on consciousness. *Neuron* 110, 1891–1893. <https://doi.org/10.1016/j.neuron.2022.05.014>.
78. Davis, Z.W., Muller, L., Martinez-Trujillo, J., Sejnowski, T., and Reynolds, J.H. (2020). Spontaneous travelling cortical waves gate perception in behaving primates. *Nature* 587, 432–436. <https://doi.org/10.1038/s41586-020-2802-y>.
79. He, B.J. (2013). Spontaneous and task-evoked brain activity negatively interact. *J. Neurosci.* 33, 4672–4682. <https://doi.org/10.1523/JNEUROSCI.2922-12.2013>.
80. Hesselmann, G., Kell, C.A., and Kleinschmidt, A. (2008). Ongoing activity fluctuations in hMT+ bias the perception of coherent visual motion. *J. Neurosci.* 28, 14481–14485. <https://doi.org/10.1523/JNEUROSCI.4398-08.2008>.
81. Hesselmann, G., Kell, C.A., Eger, E., and Kleinschmidt, A. (2008). Spontaneous local variations in ongoing neural activity bias perceptual decisions. *Proc. Natl. Acad. Sci. USA* 105, 10984–10989. <https://doi.org/10.1073/pnas.0712043105>.
82. van Dijk, H., Schoffelen, J.M., Oostenveld, R., and Jensen, O. (2008). Prestimulus oscillatory activity in the alpha band predicts visual discrimination ability. *J. Neurosci.* 28, 1816–1823. <https://doi.org/10.1523/JNEUROSCI.1853-07.2008>.
83. Wyart, V., and Tallon-Baudry, C. (2009). How ongoing fluctuations in human visual cortex predict perceptual awareness: baseline shift versus decision bias. *J. Neurosci.* 29, 8715–8725. <https://doi.org/10.1523/JNEUROSCI.0962-09.2009>.
84. Klatzmann, U., Froudist-Walsh, S., Bliss, D.P., Theodoni, P., Mejias, J., Niu, M., Rapan, L., Palomero-Gallagher, N., Sergent, C., Dehaene, S., et al. (2022). A connectome-based model of conscious access in monkey cortex. *bioRxiv*. <https://doi.org/10.1101/2022.02.20.481230>.
85. van Kempen, J., Gieselmann, M.A., Boyd, M., Steinmetz, N.A., Moore, T., Engel, T.A., and Thiele, A. (2021). Top-down coordination of local cortical state during selective attention. *Neuron* 109, 894–904.e8. <https://doi.org/10.1016/j.neuron.2020.12.013>.
86. Engel, T.A., Steinmetz, N.A., Gieselmann, M.A., Thiele, A., Moore, T., and Boahen, K. (2016). Selective modulation of cortical state during spatial attention. *Science* 354, 1140–1144. <https://doi.org/10.1126/science.aag1420>.
87. Ray, W.J., and Cole, H.W. (1985). EEG alpha activity reflects attentional demands, and beta activity reflects emotional and cognitive processes. *Science* 228, 750–752. <https://doi.org/10.1126/science.3992243>.
88. Alayrangues, J., Torrecillos, F., Jahani, A., and Malfait, N. (2019). Error-related modulations of the sensorimotor post-movement and foreperiod beta-band activities arise from distinct neural substrates and do not reflect efferent signal processing. *Neuroimage* 184, 10–24. <https://doi.org/10.1016/j.neuroimage.2018.09.013>.
89. Engel, A.K., and Fries, P. (2010). Beta-band oscillations—signalling the status quo? *Curr. Opin. Neurobiol.* 20, 156–165. <https://doi.org/10.1016/j.conb.2010.02.015>.
90. David, F., Courtiol, E., Buonviso, N., and Fourcaud-Trocmé, N. (2015). Competing mechanisms of gamma and beta oscillations in the olfactory bulb based on multimodal inhibition of mitral cells over a respiratory cycle. *eNeuro* 2. ENEURO.0018-15.2015. <https://doi.org/10.1523/ENEURO.0018-15.2015>.
91. Spitzer, B., and Haegens, S. (2017). Beyond the status quo: a role for beta oscillations in endogenous content (re)activation. *eNeuro* 4. ENEURO.0170-17.2017. <https://doi.org/10.1523/ENEURO.0170-17.2017>.
92. Miller, E.K., Lundqvist, M., and Bastos, A.M. (2018). Working Memory 2.0. *Neuron* 100, 463–475. <https://doi.org/10.1016/j.neuron.2018.09.023>.
93. Panagiotaropoulos, T.I., Kapoor, V., and Logothetis, N.K. (2013). Desynchronization and rebound of beta oscillations during conscious and unconscious local neuronal processing in the macaque lateral prefrontal cortex. *Front. Psychol.* 4, 603. <https://doi.org/10.3389/fpsyg.2013.00603>.
94. Hardstone, R., Flounders, M.W., Zhu, M., and He, B.J. (2022). Frequency-specific neural signatures of perceptual content and perceptual stability. *eLife* 11, e78108. <https://doi.org/10.7554/eLife.78108>.
95. Zhu, M., Hardstone, R., and He, B.J. (2022). Neural oscillations promoting perceptual stability and perceptual memory during bistable perception. *Sci. Rep.* 12, 2760. <https://doi.org/10.1038/s41598-022-06570-4>.
96. Jensen, O., and Bonnefond, M. (2013). Prefrontal α - and β -band oscillations are involved in rule selection. *Trends Cogn. Sci.* 17, 10–12. <https://doi.org/10.1016/j.tics.2012.11.002>.
97. Buschman, T.J., Denovellis, E.L., Diogo, C., Bullock, D., and Miller, E.K. (2012). Synchronous oscillatory neural ensembles for rules in the prefrontal cortex. *Neuron* 76, 838–846. <https://doi.org/10.1016/j.neuron.2012.09.029>.
98. Hazy, T.E., Frank, M.J., and O'Reilly, R.C. (2007). Towards an executive without a homunculus: computational models of the prefrontal cortex/basal ganglia system. *Philos. Trans. R. Soc. Lond. B Biol. Sci.* 362, 1601–1613. <https://doi.org/10.1098/rstb.2007.2055>.
99. Rougier, N.P., and O'Reilly, R.C. (2002). Learning representations in a gated prefrontal cortex model of dynamic task switching. *Cogn. Sci.* 26, 503–520. https://doi.org/10.1207/s15516709cog2604_4.
100. Lau, H., and Rosenthal, D. (2011). Empirical support for higher-order theories of conscious awareness. *Trends Cogn. Sci.* 15, 365–373. <https://doi.org/10.1016/j.tics.2011.05.009>.
101. Baars, B.J. (1997). In the Theater of Consciousness: the Workspace of the Mind (Oxford University Press). <https://doi.org/10.1093/acprof:oso/978019512659.001.1>.
102. Del Cul, A., Dehaene, S., Reyes, P., Bravo, E., and Slachevsky, A. (2009). Causal role of prefrontal cortex in the threshold for access to consciousness. *Brain* 132, 2531–2540. <https://doi.org/10.1093/brain/awp111>.
103. Qian, C., Liu, C., Zou, J., Zhuo, Y., He, S., and Zhang, P. (2018). BOLD signal modulated with perception in the superficial layer of human V1 during binocular rivalry. *J. Vis.* 18, 955. <https://doi.org/10.1167/18.10.955>.
104. Huang, Z., Tarnal, V., Vlisides, P.E., Janke, E.L., McKinney, A.M., Picton, P., Mashour, G.A., and Hudetz, A.G. (2021). Anterior insula regulates brain network transitions that gate conscious access. *Cell Rep.* 35, 109081. <https://doi.org/10.1016/j.celrep.2021.109081>.
105. Wilson, H.R. (2003). Computational evidence for a rivalry hierarchy in vision. *Proc. Natl. Acad. Sci. USA* 100, 14499–14503. <https://doi.org/10.1073/pnas.2333622100>.
106. Brascamp, J.W., van Ee, R., Noest, A.J., Jacobs, R.H.A.H., and van den Berg, A.V. (2006). The time course of binocular rivalry reveals a fundamental role of noise. *J. Vis.* 6, 1244–1256. <https://doi.org/10.1167/6.11.8>.
107. Huguet, G., Rinzel, J., and Hupé, J.M. (2014). Noise and adaptation in multistable perception: noise drives when to switch, adaptation determines percept choice. *J. Vis.* 14, 19. <https://doi.org/10.1167/14.3.19>.
108. Panagiotaropoulos, T.I., Kapoor, V., Logothetis, N.K., and Deco, G. (2013). A common neurodynamical mechanism could mediate externally induced and intrinsically generated transitions in visual awareness. *PLoS One* 8, e53833. <https://doi.org/10.1371/journal.pone.0053833>.
109. Northoff, G., and Zilio, F. (2022). Temporo-spatial Theory of Consciousness (TTC) - bridging the gap of neuronal activity and phenomenal states. *Behav. Brain Res.* 424, 113788. <https://doi.org/10.1016/j.bbr.2022.113788>.

110. Koch, C., Massimini, M., Boly, M., and Tononi, G. (2016). Posterior and anterior cortex - where is the difference that makes the difference? *Nat. Rev. Neurosci.* 17, 666. <https://doi.org/10.1038/nrn.2016.105>.
111. Mazzucato, L., Fontanini, A., and La Camera, G. (2015). Dynamics of multistable states during ongoing and evoked cortical activity. *J. Neurosci.* 35, 8214–8231. <https://doi.org/10.1523/JNEUROSCI.4819-14.2015>.
112. Tsodyks, M., Kenet, T., Grinvald, A., and Arieli, A. (1999). Linking spontaneous activity of single cortical neurons and the underlying functional architecture. *Science* 286, 1943–1946. <https://doi.org/10.1126/science.286.5446.1943>.
113. Maynard, E.M., Nordhausen, C.T., and Normann, R.A. (1997). The Utah intracortical electrode array: a recording structure for potential brain-computer interfaces. *Electroencephalogr. Clin. Neurophysiol.* 102, 228–239. [https://doi.org/10.1016/S0013-4694\(96\)95176-0](https://doi.org/10.1016/S0013-4694(96)95176-0).
114. Hussar, C.R., and Pasternak, T. (2009). Flexibility of sensory representations in prefrontal cortex depends on cell type. *Neuron* 64, 730–743. <https://doi.org/10.1016/j.neuron.2009.11.018>.
115. Safavi, S., Dwarakanath, A., Kapoor, V., Werner, J., Hatsopoulos, N.G., Logothetis, N.K., and Panagiotaropoulos, T.I. (2018). Nonmonotonic spatial structure of interneuronal correlations in prefrontal microcircuits. *Proc.Natl.Acad.Sci. USA* 115, E3539–E3548. <https://doi.org/10.1073/pnas.1802356115>.
116. Quiroga, R.Q., Nadasdy, Z., and Ben-Shaul, Y. (2004). Unsupervised spike detection and sorting with wavelets and superparamagnetic clustering. *Neural Comput.* 16, 1661–1687. <https://doi.org/10.1162/089976604774201631>.
117. Kadir, S.N., Goodman, D.F.M., and Harris, K.D. (2014). High-dimensional cluster analysis with the masked EM algorithm. *Neural Comput.* 26, 2379–2394. https://doi.org/10.1162/NECO_a_00661.
118. Hazan, L., Zugaro, M., and Buzsáki, G. (2006). Klusters, NeuroScope, NDManager: a free software suite for neurophysiological data processing and visualization. *J. Neurosci. Methods* 155, 207–216. <https://doi.org/10.1016/j.jneumeth.2006.01.017>.
119. Logothetis, N.K., Eschenko, O., Murayama, Y., Augath, M., Steudel, T., Evrard, H.C., Besserve, M., and Oeltermann, A. (2012). Hippocampal-cortical interaction during periods of subcortical silence. *Nature* 491, 547–553. <https://doi.org/10.1038/nature11618>.
120. Bokil, H., Andrews, P., Kulkarni, J.E., Mehta, S., and Mitra, P.P. (2010). Chronux: a platform for analyzing neural signals. *J. Neurosci. Methods* 192, 146–151. <https://doi.org/10.1016/j.jneumeth.2010.06.020>.
121. Oostenveld, R., Fries, P., Maris, E., and Schoffelen, J.M. (2011). FieldTrip: open source software for advanced analysis of MEG, EEG, and invasive electrophysiological data. *Comput. Intell. Neurosci.* 2011, 156869. <https://doi.org/10.1155/2011/156869>.
122. Schwarz, G. (1978). Estimating the dimension of a model. *Ann. Statist.* 6, 461–464. <https://doi.org/10.1214/aos/1176344136>.
123. Hodges, J.L., and Lehmann, E.L. (1963). Estimates of location based on rank tests. *Ann. Math. Statist.* 34, 598–611. <https://doi.org/10.1214/aoms/117704172>.

STAR★METHODS

KEY RESOURCES TABLE

REAGENT or RESOURCE	SOURCE	IDENTIFIER
Software and algorithms		
FieldTrip	https://www.fieldtriptoolbox.org/	https://doi.org/10.1155/2011/156869
Chronux Toolbox	https://www.mathworks.com/matlabcentral/fileexchange/68537-chronux-analysis-software	https://doi.org/10.1016/j.jneumeth.2010.06.020
MATLAB 2016b and MATLAB 2022a	Custom scripts for analysis written in MATLAB 2016b and 2022a have been deposited into a repository with a public license.	https://doi.org/10.5281/zenodo.7642910

RESOURCE AVAILABILITY

Lead contact

Information and requests for data and code availability should be directed to and will be fulfilled by the lead contact, Theofanis I. Panagiotaropoulos (theofanis.panagiotopoulos@tuebingen.mpg.de).

Materials availability

Materials availability does not apply here as no wet-lab work was carried out.

Data and code availability

Electrophysiological recordings used in this paper will be used in the future for other studies. Therefore, the data is available upon reasonable request; please contact the [lead contact](#). Custom analysis scripts written in MATLAB are available upon request from the co-first authors.

EXPERIMENTAL MODEL AND SUBJECT DETAILS

Two adult, male rhesus macaques (*Macaca mulatta*), weighing between 9.4–9.6kg and 12.2–12.8kg respectively, were employed in the study. The subjects, denoted as H07 and A11, were pair-housed in an enriched animal facility. They were habituated to a primate task training chair of custom design, and the experimental booth.

METHOD DETAILS

Electrophysiological recordings

We performed extracellular electrophysiological recordings in the inferior convexity of the lateral PFC of 2 awake adult, male rhesus macaques (*Macaca mulatta*) using chronically implanted Utah microelectrode arrays¹¹³ (Blackrock Microsystems, Salt Lake City, Utah USA). We implanted the arrays 1–2 millimetres anterior to the bank of the arcuate sulcus and below the ventral bank of the principal sulcus, thus covering a large part of the inferior convexity in the ventrolateral PFC, where neurons selective for direction of motion have been previously found.^{114,115} The arrays were 4×4mm wide, with a 10 by 10 electrode configuration and inter-electrode distance of 400μm. Electrodes were 1mm long therefore recording from the middle cortical layers. The monkeys were implanted with form-specific titanium head posts on the cranium after modelling the skull based on an anatomical MRI scan acquired in a vertical 7T scanner with a 60cm diameter bore (Biospec 47/40c; Bruker Medical, Ettlingen, Germany). All experiments were approved by the local authorities (Regierungspräsidium, protocol KY6/12 granted to TIP as the principal investigator) and were in full compliance with the guidelines of the European Community (EUVD 86/609/EEC) for the care and use of laboratory animals.

Data acquisition, spike sorting and local field potentials

Broadband neural signals (0.1–30 kHz) were recorded using Neural Signal Processors (NSPs) from Blackrock Microsystems Inc. Signals from the Utah array were digitised, amplified, and then routed to the NSPs for acquisition via CerePlex E headstages and the corresponding pre-amplifiers. For the offline detection of action potentials, broadband data were filtered between 0.6 and 3 kHz using a second-order Butterworth filter (the filter was chosen such that it allowed a flat response in the passband while contributing the

least phase distortion due to its low order, yet having an acceptable attenuation in the stop band, i.e. a roll-off starting at -20dB). The amplitude for spike detection was set to five times the median absolute deviation (MAD).¹¹⁶ Spikes were rejected if they occurred within 0.5 ms of each other, (multi-unit refractory period temporal threshold) or if they were larger than 50 times the MAD (to exclude large motion artifacts). All collected spikes were aligned to their minimum. Automatic clustering to detect putative single neurons was performed by a Split and Merge Expectation-Maximisation (SMEM) algorithm that fits a mixture of Gaussians to the spike feature data which consisted of the first three principal components¹¹⁷ (Klustakwik). The clusters were finalised manually using a cut-and-merge software¹¹⁸ (Klusters). For the analysis of LFP activity, the broadband signal was decimated to 500 Hz sampling rate using a Type I Chebyshev Filter, reliably preserving frequency components up to 200 Hz.

Visual stimulation and experimental paradigm

Visual stimuli were generated by in-house software written in C/Tcl and used OpenGL implementation. These stimuli were displayed using a dedicated graphics workstation (TDZ 2000; Intergraph Systems, Huntsville, AL, USA) with a resolution of 1,280 × 1,024 and a 60Hz refresh rate. An industrial PC with one Pentium CPU (Advantech) running the QNX real-time operating system (QNX Software Systems) controlled the timing of stimulus presentation, and the digital pulses to the electrophysiological data acquisition system. Eye movements were captured using an IR camera sampling at 1kHz, using the software iView (SensoriMotoric Instruments GmbH, Germany). They were monitored online and stored for offline analysis using both the QNX-based acquisition system and the Blackrock data acquisition system. We were able to reliably capture the eye movements of the animals by positioning the IR camera in front of a cold mirror stereoscope.

Initially, the two monkeys (A11 and H07) were trained to fixate on a red square of 0.2° of visual angle about 45cm away from the monitors that could be viewed through the stereoscope. This dot was first presented in one eye, (the location of the red fixation square was adjusted to the single eye vergence of each individual monkey) and the eye-position was centred using a self-constructed linear offset amplifier. While the monkey was fixating, the dot was removed and immediately presented in the other eye. Over multiple presentations, the offset between the two eyes was averaged to provide a horizontal correction factor to allow the two dots to be perfectly fused within the resolution limitations of the recording device (1/100th of a degree). The monkeys were trained to maintain fixation within a window of 2° of visual angle during initiation. After 300ms of fixation, a moving grating of size 8°, moving in the vertical direction (90° or 270°) at a speed of 12° (monkey H) and 13° (monkey A) per second, with a spatial frequency of 0.5 cycles/degree of visual angle and at 100% contrast was presented for 1000–2000ms, in the first five experimental sessions. In the sixth session, 200 random dots at 100% coherence with a limited lifetime of 150ms were presented. This marked the first monocular stimulus epoch in both conditions, viz. Binocular Rivalry (BR) and Physical Alternation (PA). At the end of 1–2s, the second stimulus with the same properties as above but moving in the opposite direction was presented to the other eye. In the BR trials, this marked the “Flash Suppression” phase. These two competing stimuli were allowed to rival against each other for a period of 6–10s. In the PA trials, switches in the percept were mimicked by alternatively removing one stimulus based on the mean dominance time computed from the Gamma Distributions (tailored to each monkey’s performance and statistics) acquired during multiple training sessions, and adjusted to be closer to a mean of 2s. Free viewing within the +/-8° window, which included the stimulus, elicited the Optokinetic Nystagmus (OKN) reflex concomitant to the perceived direction of motion which served in lieu of a voluntary report, fulfilling the criterion of a “no-report paradigm”. The monkeys were given a liquid reward (either water or juice) at the end of the trial, if their fixation and eye-movement range successfully remained within the specified viewing window during the entire duration of the trial. Every successful trial was followed by a 2–2.5s inter-trial period.

Detection of spontaneous transitions

The recorded eye-movement signal in the Y-coordinate was first low-pass filtered using a 3rd order Butterworth Filter below 20Hz to remove involuntary jitter-induced high-frequency noise. A custom GUI written in MATLAB allowed us to manually identify the end of a dominance period and the beginning of the subsequent one. Manual marking (performed by two authors, AD and VK) was necessitated due to the large variability in the shapes that comprised the OKN complex. These events were based on the change in the slope of the slow-phase of the OKN. Such spontaneous switches were identified by the difference in the end of a dominance and the beginning of the next one; specifically, if this difference was less than 250ms (a fast switch). A “clean” transition was designated if the previous dominance and the subsequent one lasted for at least 500ms without being broken. Analogous to subjective reports, we aligned the LFP and the spiking activity at the beginning of the subsequent dominance period. This was performed in the same way for both BR and PA trials.

Treatment of the LFP data

Firstly, the raw decimated LFP signal (0.1–500Hz) was collected around each clean transition. A threshold 3.5 times the SD of the Gaussian noise was set and both positive and negative deviations before and after the switch were detected. Next, the LFP signal was decomposed into a time-frequency representation using a Continuous Wavelet Transform (CWT, MATLAB 2016b) with a Morse wavelet of 7 cycles. This allowed us to resolve 169 frequencies from 0.5 to 256 Hz (500 Hz sampling rate) while preserving the full temporal resolution. The CWT for each channel in each transition in each condition (BR, PA, PM and SD) was first z-scored in the frequency domain to visualise the relative changes in power and then pooled across all channels and averaged. The power spectrum to assess aperiodic and periodic components was computed by collapsing the CWT in time. To visualise the differences between

spontaneous transitions, piecemeals and randomly-triggered periods, the latter two spectrograms were subtracted from the former, respectively.

To understand the evolution of the LFP activity, we first filtered the broadband LFP trace into two constituent bands that were identified to be modulated during the task from the time-frequency analysis and the power-spectrum, i.e., the LF (1-9 Hz) and the beta band (20-40 Hz). We used a 4th and 8th order Chebyshev Type I filter respectively, with a maximum passband ripple of 0.001dB. To obtain the instantaneous amplitude in time, we transformed the signal into the Hilbert space and then computed the absolute value. Events were detected at each transition in each channel using a threshold which was 4 times the standard deviation of the noise modelled as a Gaussian distribution. The minimum duration of each event to be detected was set as one full cycle of the highest frequency in that band, i.e. 111ms for the 1-9 Hz band and 25ms for the 20-40 Hz band.¹¹⁹ The event-rate in time was computed as a quasi-PSTH by turning the detected events into a binary spike-train and smoothed with a Gaussian kernel of width 25ms, and then averaged across all channels (events/s/transition). The event-rate was computed as the sum of LF events normalised by the number of transitions and channels (events/transition/channel). To compute the build-up in the LF activity, the amplitude at each detected time-point was averaged first across all channels for a given transition, and then averaged across all transitions. A line was then fit to this mean scatter-plot using the CurveFit Toolbox in MATLAB.

Construction of direction of motion specific neural ensembles

Single neuron selectivity was assessed during perceptual transition periods of binocular rivalry (perceptual switches) and physical alternation (stimulus switches). During binocular rivalry trials, these periods were selected according to the following criteria: 1. Perceptual dominance (judged from the OKN signal) must be maintained for at least 1s post a perceptual switch 2. A preceding perceptual dominance for the competing stimulus must be maintained for 1s, and finally 3. The delay between the end and the beginning of the two dominance phases was not more than 250 milliseconds. For physical alternations, we selected trials, wherein a stimulus was presented for at least 1s before and after a stimulus switch. The spiking activity was triggered at the beginning of a forward dominance (BR) and stimulus change (PA).

Selectivity was assessed by comparing the distributions of the total number of spike counts across trials where the upward drifting grating was perceived, post (0 to 1s) or pre-switch (-1 to 0s), with trials where a downward drifting grating was perceived. We used a Wilcoxon rank sum test and all neurons where $p < 0.05$ were considered as selective. For a given transition, spikes were binned in 50ms bins for each selective neuron, and the resultant spike-count histograms were summed across the neurons that make up each selective ensemble to represent a population vector.

For the decoding analysis, LFP events in both the LF and beta range were rasterised and sorted by switch type, i.e. preferred to non-preferred and non-preferred to preferred, depending on the ensemble they were detected at. These data, along with the binned spiking data were fed into a Support Vector Machine based binary classifier (linear regression), and the decoding accuracy (area under the curve of the receiver operator characteristic – AUCROC) was computed in each 50ms bin, with an overlap of 100ms. Significance testing was achieved by shuffling the labels ($n=100$), with chance decoding at 0.5 (50% accuracy). Finally, to estimate the start of the change in encoding from the spiking activity, a piecewise linear function with 2 degrees of freedom was fit to each transition profile. The earliest detected changepoint was collected as the start time of change in encoding.

To analyse the crossover times between the two competing populations, we computed the trend in these normalised direction-selective population sum PSTH activity for every transition in a 0.9s window around the time of the marked smooth pursuit OKN change [-0.9s to 0.9s] by smoothing the raw ensemble population vectors for the two competing populations using a LOWESS filter. Next, we detected each intersection between these two given vectors using standard interpolation. Where multiple intersection points were detected, only that point was considered which was followed by divergences for a minimum of 200ms before and after the intersection point, denoting distinct encoding of the currently active percept. Finally, all cross-over times either less than -0.75s or more than 0.75s were discarded as these were considered to come from noisy trials.

Spike-field Coherence

The spike-field coherence (SFC) was computed between the spiking activity of selective ensembles for each transition, and the average LFP recorded at these selective electrodes. A rate adjustment and a finite-size correction was applied before computing the SFC via a multi-taper method¹²⁰ (Chronux Toolbox). The mean angle of spike-LFP locking was computed using the pairwise phase consistency method implemented by FieldTrip Toolbox.¹²¹

Treatment of resting-state activity

LFPs from two continuously-recorded resting state sessions on days when no task-recording was performed, were decimated to 500 Hz as mentioned above. In each channel, the beta bursts were detected using the previously-mentioned LFP event-detection algorithm. The mean of the inter-event interval was used as a threshold to decide which collection of events constituted a phase of sustained activity. These epochs were collected across all channels and pooled across the two monkeys. Both a gamma and an exponential distribution were fit to the observations and their respective AIC (Akaike Information Criterion) and BIC (Bayesian Information Criterion) measures were computed to evaluate the goodness-of-fit.¹²²

Statistical analysis

All statistical comparisons were performed using a Wilcoxon ranksum test¹²³ due to the non-gaussian nature of the underlying distribution from which the data originated (unless specified otherwise). Distributions were fit using the MATLAB statistical toolbox using a Maximum-Likelihood-Estimate method. For model comparisons, the allFitDist.m toolbox was used that also generated metrics for appropriate model selection. For non-parametric fitting of distributions with widely different sample numbers, the kernel density estimate method implemented in the MATLAB Statistics Toolbox was used to generate the best-fit function, which was then normalised for visualisation. For computing significant phase angles of spike-LFP coupling, the Rayleigh Test for circular data was used.